QUATERNARY MEGAPALEOLAKE SYSTEM IN NORTHWEST BOTSWANA: EVIDENCE OF LACUSTRINE DEPOSITION AND GEOGRAPHICAL EXTENT USING MULTIPLE GEOCHEMICAL PROXIES

By

CHARITY KGOTLAEBONYWE

Reg. No: PC14100002

BSc (Geology) (UB)

Department Of Earth and Environmental Sciences

Faculty of Science

Botswana International University of Science and Technology

charity.pema@studentmail.biust.ac.bw, (+267) 71579435

A Thesis Submitted to the Faculty of Science in Fulfilment of the Requirements for the Award of the Degree of Master of Science in Geology

BIUST

Supervisor: Dr Loago Molwalefhe

Department of Earth and Environmental Sciences,

Faculty of Science, BIUST

molwalefhel@biust.ac.bw, (+267) 71234975

Signature:  Date: 21/10/2020

October, 2020

DECLARATION AND COPYRIGHT

I, **Charity Kgotlaebonywe,** declare that this thesis is my own original work and that it has not been presented and will not be presented to any other university for a similar or any other degree award.

Signature……

CERTIFICATION

The undersigned certifies that s/he has read and hereby recommends for acceptance by the Faculty Of Science a thesis titled: **QUATERNARY MEGAPALEOLAKE SYSTEM IN NORTHWEST BOTSWANA:EVIDENCE OF LACUSTRINE DEPOSITION AND GEOGRAPHICAL EXTENT USING MULTIPLE GEOCHEMICAL PROXIES**, in fulfillment of the requirements for the degree of Master of Science in Geology of BIUST.

Dr Loago Molwalefhe

Date: 21/10/2020

ACKNOWLEDGEMENTS

I am heartily thankful to my supervisor, Dr Loago Molwalefhe, whose encouragement, guidance and support from the initial to the final stages of this work enabled me to develop an understanding of the subject matter.

I owe my deepest gratitude to Dr Eliot Atekwana of the University of Delaware, USA for the sample analyses.

Lastly, I offer my regards and blessings to all my family members who supported me in any respect during the completion of the project.

ABSTRACT

Reconstruction of climate dynamics in southern Africa has been immensely constrained by the absence of continuous proxies records. Sediments provide potential sources of studying past environments because their makeup is a direct response to variabilities in the environment and climate. In this study a multiple geochemical proxy approach was used to investigate two 30 m deep sediments cores from northern Botswana to construe their various geological processes and environments of deposition. Based on these proxy studies two distinct but dissimilar hydrological and climatic settings were identified on the two cores. For BH 11 lithological studies reveal a sediments sequence that has a bottom unit with several repetitive and alternating layers of sand-silt-clay, and a dominantly silty/clayey unit at the top. This arrangement of units likely indicates lake-related processes with input from regional rivers. Magnetic susceptibility measurements indicate a dual source of the sediments. Sediments in the lower unit (30 to 7 m depth) could have come from a distal sub-tropical source with rocks that are richer in magnetic minerals. Sediments in the upper section (from 7 m depth to surface) were strongly influenced by a more felsic source that was likely of local surrounding landscapes. Carbon dynamics in the middle portions of the lower unit of BH 11 suggests deposition under more humid conditions than in the upper section, within a periodically drying out fluvial system. Isotopically lighter $\delta^{13}C_{org}$ values (-26 to -28 ‰) for the lower section compared to the upper section (~ -20‰) reflect difference in the vegetation cover, moisture conditions and probably climate between the two sections. For core BH 10, sediments in the lower unit were sourced locally from a less magnetic and humid landscape. The upper unit signifies continually drying up condition to present day. The two sites may have hosted major lakes at different times in the past.This study validates the effectiveness of sediments in unravelling environmental and climate change in fluvial-lacustrine depositional settings, and gives the possibilities of connecting the sediment record to regional stratigraphic markers.

LIST OF FIGURES

LIST OF TABLES

TABLE OF CONTENTS

CHAPTER 1

1.0 Introduction

Research into the paleoenvironments of southern Africa started to intensify some four decades ago. A major impediment is in the discontinuity and low resolution in the paleoenvironmental records. This has continued to place a major constraint on proxy-based reconstruction of environmental and climate change in regional Quaternary studies (Knight and Fitchett, 2019). Therefore, there is a need for more records to improve correlations of regional and global climate dynamics. During the Quaternary, the climate in Southern Africa is known to have alternated between drier and wetter periods due to the latitudinal migration of the Intertropical Convergence Zone (ITCZ) (Truc et al., 2013). Sediments would preserve the environmental and climate conditions under which they formed and this particular property makes them a unique proxy for palaeoenvironmental reconstruction of depositional environments.

In the middle Kalahari region of northern Botswana (Figure 1) there exists extensive geomorphological evidence for large paleolakes which formed during historically wet climate (Grove, 1969; Shaw, 1985; 1988; Thomas and Shaw, 1991; 2002). Previous studies on the paleoclimatology of the middle Kalahari mainly focused on paleolakes geomorphology and shallow sediments geochemistry of Lake Ngami (Shaw, 1985; Shaw et al., 2003; Huntsman-Mapila et al., 2006; Burrough et al., 2007), Lake Mababe (Shaw, 1985; Burrough and Thomas, 2008; Gamrod, 2009; Teter, 2009;) and Lake Makgadikgadi (Thomas and Shaw, 1991).

Burrough and Thomas (2008) proposed that these paleolakes might have coalesced into a single large megalake Kalahari during humid periods (Figure 1). Dating of megalakes in the Kalahari shorelines yielded ages of high lake levels between 8.5ka-104.6ka (Burrough and Thomas, 2008; Burrough et al., 2007, 2009). During the Quaternary the middle Kalahari region has undergone climatic changes influencing the hydrology and associated sedimentary processes. Paleohydrological relicts, mainly Paleolake bodies were studied and associated to wetter climatic periods.

The Okavango rift zone (ORZ) is an incipient continental zone system that hosts the Okavango Delta (Figure 1), which is a classic example of how rifting could impound rivers and affect their flow patterns and sedimentation (Gumbricht et al.,2001;

Ringrose et al., 2002; Kinabo et al., 2007; Moore et al., 2012). The younger ORZ has impounded and diverted the Okavango River whose inflow used to maintain the formerly thriving Makgadikgadi megapaleolake downstream at its lower reaches (Burrough et al., 2009), to form the present day Okavango Delta. In the Cretaceous and Cenozoic prior to the initiation of rifting in the northwest Botswana, the main drainage direction was southerly and the Okavango River terminated in the Makgadikgadi megapaleolake (MPL). The disruption in the drainage of the Okavango River upstream of MPL caused massive decreases in the downstream water budget that used to supply the Makgadikgadi megapaleolake, as water was now diverted into the newly forming Okavango Delta (Gumbricht et al., 2001; Moore et al., 2012). More than 90% of inflow to the delta is currently lost to evapotranspiration and the remainder leaves as surface or groundwater flow (McCarthy et al., 2002). The impounding of the river (~41 ka) by upstream Thamalakane and Kunyere faults (Figure 1) to form the Delta further diverted downstream supply. This led to contractions of the MPL that eventually perished into the highly saline and alkaline present-day Makgadikgadi Salt Pans.

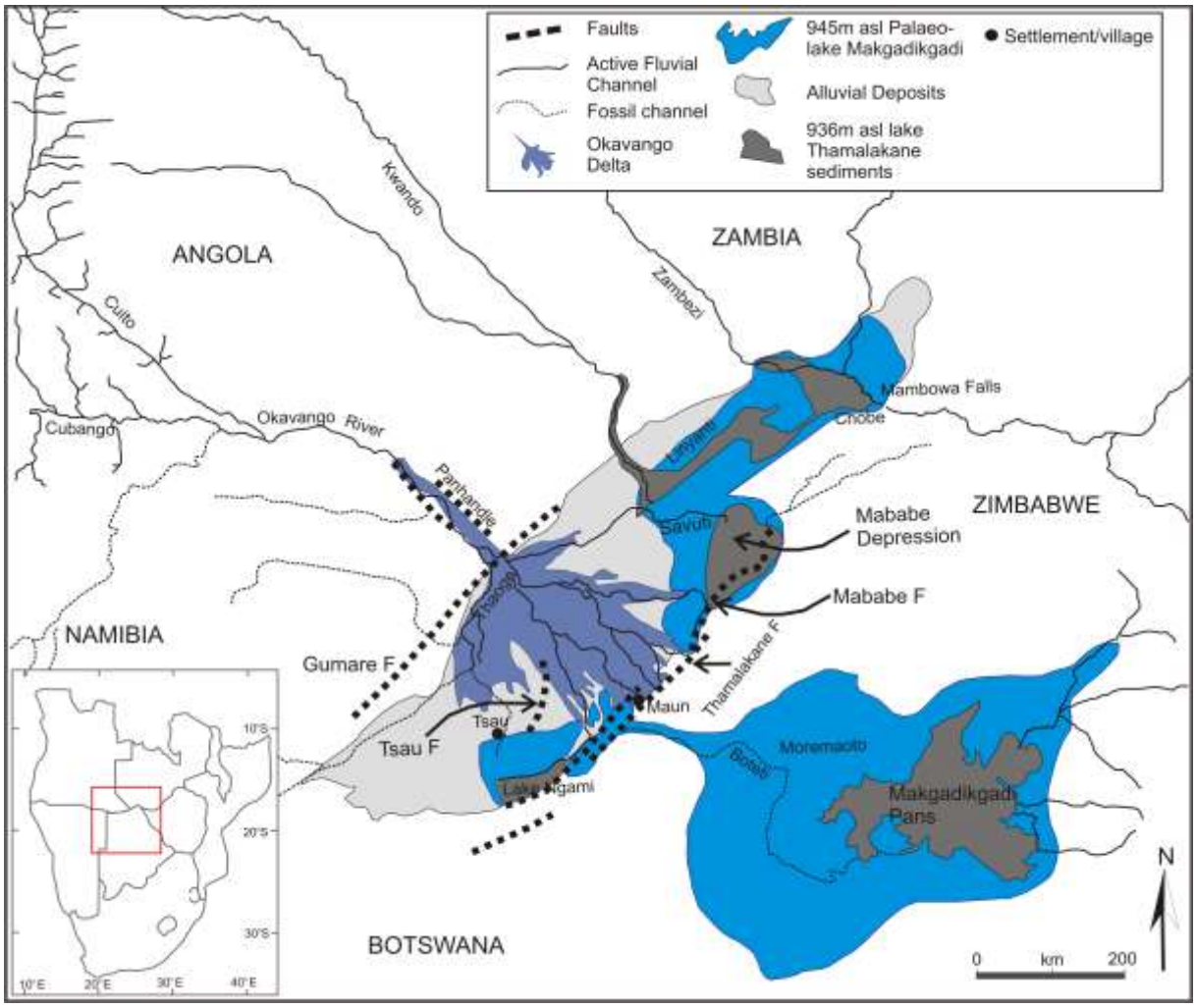

Figure 1: The Okavango Rift Zone and the projected extent of the middle-Kalahari Quaternary megapaleolake system in northern Botswana (modified from Burrough and Thomas, 2008).

Additional to the formation of the Delta due to continued regional faulting, other fault-controlled depressions of Mababe and Ngami sub-basins were developed and constitute the landscape of today's northwest Botswana (Gumbricht et al., 2001; Kinabo et al., 2007).

In the Pleistocene, the MPL has had a history of lake level fluctuations related to moisture budgets and regional climate variations in southern Africa (Thomas and Shaw, 2002). During times of high inflows the endorheic megalake occupied a larger part of the land as lake levels rose to reach the contour elevation of 945 m.a.s.l. (Shaw, 1988), covering an area of approximated at 66 000 km^2, making the MPL one of the largest lakes in the world. On the other hand, lake contractions have taken lake levels

to as low as 936 m.a.s.l. (Moore et al., 2012), which formed the younger Lake Thamalakane (Shaw, 1988) with distinct shorelines (Figure 1).

With further depression due to tectonism the delta continued to develop and deposited mainly sand sediment load to a depth of over 200 m onto the older underlying subsided regional sequence of the Kalahari Beds that overly the Karoo sedimentary system (Gumbricht et al., 2001).

In summary, the modern MPL of is permanently desiccated lake was a result of two totally contrasting hypotheses; (1) sequential river capturing due to rifting in the upstream sections of the Okavango River (2) climate controlled evaporation of the MPL, or maybe a combination of both hypotheses (1) and (2). The complex geological record of tectonism and both wet and dry contrast in climate, which influenced lake levels in the past are likely preserved in the sediments record of the Okavango Delta, the Makgadikgadi Basin and other megapaleolake localities. This sediment record is fundamental to reconstruct and understand the dynamic past and present environments of the northwest of Botswana.

1.1 Aims and Objectives

The project is aimed at reconstructing and understanding of past hydrologic regimes of the northwest part of Botswana from analyses of sedimentological and geochemical datasets during the Quaternary. The project objective is to qualitatively evaluate relationships between physical and chemical properties of sediments and assess past hydrologic regimes, from areas between the 945 m.a.s.l and 936 m.a.s.l. contour lines. To meet the project objectives, physical properties of sediments will be evaluated for provenance, and geochemical proxies will be used to document hydrologic, environmental and climate variability.

1.2 Hypothesis

The hypothesis that drives this research is that if the climate is drying, organic carbon biomass must dwindle, carbon isotopic composition becomes more positive compared to a wetting climate which would have more organic carbon biomass with more negative carbon isotopic composition.

1.3 Significance of the study

The presence of lacustrine deposits within the sedimentary record in the lower Okavango Delta may confirm the existence of a continuous body of water that extended to join the Lake Mababe Depression, Lake Ngami and the Makgadikgadi Basin into one megapaleolake Makgadikgadi. The presence of megapaleolake in this region is important for predicting future ramifications that are due to anthropogenic climate change and affect infrastructure and human safety, settlements and social and economic activities in the region (Hamandawana et al., 2008). Flooding from large lakes can affect plant and animal communities that exist in the area by altering the hydrologic regime. Also, information on past hydrologic conditions and understanding of the creation and demise of large megapaleolakes in this area can also be useful for future socio-economic planning and management of vast resources of the Okavango Delta (Thomas and Shaw, 1991). The data from this research can be incorporated into rainfall and flooding models of the area which can help predict landscape changes due to climate change. This study will also advance discovery and understanding in the field of paleoenvironmental investigations in Okavango Delta during the Quaternary and later.

1.4 Justification of the study

Surficial processes in the Okavango Delta have been deduced mainly from geophysical studies, geomorphology and the relationship between relief and tectonics setting (Kinabo et al., 2007; Gumbricht et al., 2004), provenance and geochemistry of sediments (Huntsman-Mapila et al., 2005), and micro-topography (McCarthy et al., 2012). Defining regional paleo-environment of the Okavango Delta from a geochemical perspective is clearly lacking, but of competing primary significance. It is critical to understand the evolution (creation and demise) of megalakes in terms of surface processes such as climate change, biodiversity evolution and hydrological variations over geological time frames.

For the first time, this study seeks to (i) characterize samples from deeper sediments sequence using their lithological, magnetic properties geochemical composition and isotopic content; and ii) establish inferences of paleo-environments and paleo-climates using these data.

CHAPTER 2

2.0 Literature Review

2.1 Background information

As a consequence of erosion, transportation and deposition of sedimentary materials different depositional environments may possess distinctive physical and chemical characteristics that may make it possible to elucidate the environment of deposition and thus utilise the physical and chemical properties of sediments as tools for paleoenvironmental reconstruction (Lario et al, 2002). Recent research highlighted the potential for sediment sequences in lakes to act as archives of flooding of different magnitudes and over different timescales (Schillereff et al., 2014). Studies of past environments may give insight into potential future environmental changes which could allow for development of model scenarios to evaluate anthropogenic forcing on local environments (Robinson and Dowsett, 2010). These investigations also have implications for human evolution and dispersal, such as identifying key events forcing evolution and plotting migration routes based on past landscapes (Thomas and Burrough, 2012).

Reconstructions of past environments are based on a range of proxy data from marine and terrestrial records. Other considerations for paleoenvironmental reconstructions are based on the interpretation of geomorphology as relict landforms in the form of lake shorelines, sediments and sand dune systems (Thomas and Burrough, 2012). Lakes accumulate sediments continually. The sediments may consist of biological remains from lake itself and its surroundings, as well as soil particles and other non-biological material originating from the lake catchment as well as from atmospheric fallout.

Sediment plumes entering lakes are subjected to a number of physical and chemical processes that determine the nature and rate of deposition across the lake bed (Schillereff et al., 2014). Materials extracted from a lake bed are typically composed of clastic sediments as well as biogenic compounds that may include silicates, carbonates and organic matter (Lowe and Walker, 1997). Paleoflood records are most effectively obtained from sediment sequences where river-borne material is delivered

during a flood to overprint the near-continous autogenic (internal) or allogenic (external) sedimentation pattern at the lake bed with a distinctive detrital lamination (Schillereff et al., 2014). When paleoflood records are extracted from different lake settings, site specific hydrogeomorphic processes, sediment provenance and depositional mechanisms must be considered (Schillereff et al., 2014).

Catchments with considerable erodible soil cover and limited interruption of the sediment conveyor in the form of large deltas or extensive floodplains will receive greater allochthonous input (Dearing, 1997) and are therefore better suited to paleoflood reconstruction (Foster et al., 2008; Parris et al., 2010).

2.1.1 Middle Kalahari geomorphological evidence

The Kalahari Desert of southern Africa has an environment of great ecological and geomorphological diversity, a complex climatic and geological history and a long association with human societies (Thomas and Shaw, 1991). Fluctuating climatic conditions have created the need for intensive research on the environmental impact of changing hydrologic budgets of past climates (Fields, 2012). One such environment of changing hydrologic budgets is southern Africa's largest wetland, the Okavango Delta, situated in the middle Kalahari in northwest Botswana, and is one of only two perennial sources of water in Botswana (McCarthy and Ellery, 1998).

The appearance and disappearance of megapaleolakes in the past indicated significant variability in the hydrological conditions of the middle Kalahari and thus warrants a need for research on varying environmental conditions to better understand the past environmental dynamics of the region which is a requisite for understanding and predicting future hydrologic changes.

Evidence for wet climate and the spatial extent of the megapaleolakes Makgadikgadi and Thamalakane have been derived primarily from geomorphologic studies based on elevations of lake highstands (Shaw, 1988; Thomas and Shaw, 1991; 2002), and from age estimates using beach ridge sediments and sediment analyses (Thomas and Burrough, 2011). These studies used sedimentological and geochemical signatures to identify the timing of mega-lake formation and their hydrologic and sedimentological evolution.

The spatial coverage of the megapaleolake proposed by previous studies (Shaw, 1988; Thomas and Burrough 2012) suggest that lacustrine sediments should be found at elevations as high as 945 m a.s.l, an area that encapsulates the lower Okavango Delta and the Makgadikgadi Pans complexes (Figure 1). It is unclear why all previous researches related to megapaleolakes in Botswana have been conducted within the margins of present day lake basins, yet the mega-lakes have been presumed to extend beyond such margins, save for the Kalahari sands acting as an inhibitor. Both Lake Ngami and Mababe Depression (Figure 1), contain concentric patterns of beach ridges and shorelines indicating former lakes extending to 1800 km^2 at Ngami and 3000 km^2 at Mababe (Shaw, 1985). The present day Makgadikgadi Basin is a much larger lake basin and has a surface area of 37,000 km^2 (Shaw, 1988). If the paleolake Makgadikgadi spanned 66,000 km^2 (Burrough et al., 2009), then the scope for the search of the spatial occurrence of the megapaleolake needs to be broadened to cover areas beyond the current lake margins. Understanding of the presence, extent and duration of the mega-lakes can be improved by investigating the sedimentary record and examining lacustrine sedimentation beyond the margins of Makgadikgadi Basin, Lake Ngami and the Mababe Depression.

Studies on hydromorphological and paleolimnological development of the Makgadikgadi Basin during the last 50 ka, suggest that from c.46-16 ka the Makgadikgadi megapaleolakes did not receive water from the Okavango River in the north, but from paleo-rivers located in the south-western catchment (Riedel et al., 2014). Studies on a 30 cm thick sediment unit in the Gidikwe Ridge (Schidmt et al., 2017) concluded that the unit covers a period of not more than 1 ka, with a temporal resolution of the samples of 1-2 decades. The study also gave information that 30 cm is too short to give an insight into the climate variability during the megalake phase. OSL dates (100 ka) suggest that the megalake in the Kalahari occurred during an extremely arid climate (MIS 5) though there were some short excursions to more humid conditions during cold-warm and warm-cold transitions.

Although the studied megalake period was likely a short term climate anomaly possibly triggered by North-Atlantic iceberg discharges, it is challenging the view that MIS 5 was mostly extremely dry. That the environment may have hydrologically been more favourable, is supported by archaeological and genetic data suggesting permanent

human occupation of the Kalahari since MIS 5 (Pleistocene).Understanding the spatiotemporal context of lake development in the depressions of the MOZB has further been hampered by the problem of proper dating. Riedel et al 2014, added six periods of lake development which mostly happened during MIS 3 (59-24 ka) and MIS 2 (24-12 ka). The development of Paleolake Makgadikgadi during the last 50 ka is characterized by strong lake level fluctuations and thus substantial limnological changes at different time intervals. The durations of lake high stands remain unclear but may lie in a range of decades to millennia.

2.2 Lake sediments as climate archives

Lakes are efficient preservatory sites for clastic material eroded from catchment slopes and floodplains that subsequently get transported through the river systems (Markereth, 1966; Oldfield, 2005), hence keeping a continuous and cumulative record of the hydrodynamic and biochemical conditions of the watershed and the lake environment. If the hydrodynamic relationships between river discharge and entrainment potential of various particle sizes is reflected in the materials received by the lake basin and incorporated into the sediment record, then high magnitude river flows should appear as distinct layers of coarse material, whereas low magnitude flows are preserved in the form of layers of fine grained materials.

Sediments obtained from a lake bed are typically composed of clastic (i.e., terrestrially-derived) material as well as autochthonous biogenic compounds that can include silicates, carbonate and organic matter (Lowe and Walker, 1997). Lakes often keep a sediment mix consisting of fine-grained allochthonous clay and silt, siliceous material (e.g., diatoms) and variable organic matter content, composed of detrital plant material (leaves, wood, seeds) and humic substances as well as autogenic planktonic and benthic microbes (Håkanson and Jansson, 1983; Lowe and Walker, 1997).

The sediments may consist of biological remains from the lake itself and its surroundings, as well as soil particles and other non-biological material originating from the lake catchment as well as from atmospheric fallout. Hence, sediment sequences in lakes contains information about the history of the lake and its surroundings.

Sediment plumes entering lakes are subjected to a number of physical and chemical processes that determine the nature and rate of deposition across the lake bed

(Schillereff et al., 2014). Materials extracted from a lake bed are typically composed of clastic sediments as well as biogenic compounds that may include silicates, carbonates and organic matter (Lowe and Walker, 1997). Paleoflood records are most effectively extracted from sediment sequences where river-borne material is delivered during a flood to overprint the near-continous autogenic (internal) or allogenic (external) sedimentation pattern at the lake bed with a distinctive detrital lamination (Schillereff et al., 2014). When paleoflood records are extracted from different lake settings, site specific hydrogeomorphic processes, sediment provenance and depositional mechanisms must be considered (Schillereff et al., 2014).

2.3 Paleoenvironmental proxies

Integrating multiple paleoenvironmental proxies offers a comprehensive approach to studying the various components of the sediments make-up and a better understanding of changes in fluvial dynamics, landscape erosional patterns and sediment supply as well as identifying shifts in the climate–vegetation–soil relationship (Koinig et al., 2003). For instance, pollen and plant macrofossil records will reflect changes in vegetation cover hence may be used as indicators for provenance and hydrologic regime changes (Dearing and Jones, 2003). Charcoal trapped in sediments can indicate past fire events. Remains of organisms such as diatoms, foraminifera, microbiota, and pollen within sediment can indicate changes in past climate, since each species has a limited range of habitable conditions. When these organisms and pollen sink to the bottom of a lake or ocean, they become buried within the sediment. Thus, climate change can be inferred by species composition within the sediment.

2.3.1 Chemical Proxies

Inorganic and organic geochemical measurements also provide insights into catchment soil development and weathering and erosional processes (Giguet-Covex et al., 2011) that may influence sediment supply through time.

2.3.1.1 Total Organic Carbon (TOC) and Total Inorganic Carbon (TIC)

TOC concentrations is a bulk value that represents the fraction of organic matter that escaped remineralization during sedimentation. The particulate detrital material from plants that live in water and on the land surrounding lakes would make up the primary source of organic matter to lake sediments (Meyers and Ishiwatari, 1993). However, during the filling of Paleolake Makgadikgadi, organic matter would have been

transported from both the Angolan catchment and from wetland vegetation around the lake.

Organic matter in lake sediments is a mix of aquatic and terrestrial plant debris, the latter resulting from watershed erosion (Meyers and Teranes 2002). The organic matter content may thus be useful in reconstructing paleoenvironments of lakes and their watersheds and to infer past regional climate changes (Brenner et al., 1999). In arid and semi-arid areas, regional moisture is the main factor influencing plant growth. In humid climates, plants grow vigorously, leading to a higher content of organic matter in lake sediments, whereas under arid conditions, plant growth is limited and organic matter content in lake sediments is also lower. The lower organic matter content indicates drier climate period, while the higher organic matter content reflects wetter climate intervals (Liu et al., 2002; Wu et al., 2009; Oldfield et al., 2010; Zhong et al., 2010).

2.3.2 Carbon Isotopic composition

The carbon isotope of bulk organic matter depends on several factors, such as sources of organic matter, biological productivity within the lake, intensity of photosynthesis, hydrological conditions, sediment environment, and preservation of lake sediment (Hayes, 1993; Kump and Arthur, 1999; Wu et al., 2007).

The carbon stable isotopic composition ($\delta^{13}C$) of organic matter in lake sediments is controlled by several factors including the contribution of various sources (algal, terrestrial) and changes in the respective photosynthetic pathways, changes in aquatic productivity, and the $\delta^{13}C$ of dissolved inorganic carbon (DIC) inputs to a lake (Meyers and Ishiwatari, 1993; Meyers and Teranes, 2001; Finney et al., 2012).

Changes in the $\delta^{13}C$ of dissolved CO_2 supplied to Alaskan lakes have been shown to influence the $\delta^{13}C$ of sedimentary organic matter (Finney et al., 2012). Many Alaskan lakes have surface water pCO_2 concentrations above atmospheric levels, due to inputs of watershed respired CO_2 from permafrost or organic rich soils (Kling et al., 1991). In such lacustrine systems, increased inputs of watershed respired CO_2 with relatively low $\delta^{13}C$ values typical of C_3 plants (~-27‰) results in relatively low $\delta^{13}C$ organic matter content (Finney et al., 2012).

Inorganic carbon isotope ratios mainly from the bicarbonate species (HCO_3^-), Dissolved Inorganic Carbon (DIC) in lake waters are useful as tracers of environmentally determined processes that often relate to climate variability (Meyers, 2003). Carbon isotopes are fractionated during various carbon transformations that ultimately get incorporated into authigenic and biogenic carbonates. The bicarbonate is derived from interaction of groundwaters with rocks and soils in the catchment. In general there are three predominant processes that control the inorganic carbon isotope composition of the DIC in lacustrine environments; the isotopic composition of the inflowing waters, CO_2 exchange between atmosphere and lake water, and photosynthetic nature of aquatic plants within the lake.

The carbon isotopic composition of organic matter in lake sediments is important to assessing organic matter sources, for reconstructing past productivity rates, and for identifying changes in the availability of nutrients in surface waters. Increases in the accumulation rates of organic matter and its $^{13}C/^{12}C$ ratio ($\delta^{13}C$) have been used widely as an indicator of enhanced aquatic productivity in lakes (Hollander and McKenzie, 1991; Hollander et al., 1992; Hodell and Schelske, 1998; Brenner et al., 1999). Phytoplanktons (C_3 algae) preferentially utilize ^{12}C to produce organic matter that averages 20‰ lighter than the ($\delta^{13}C$) of their dissolved inorganic carbon (DIC) source (O'Leary, 1988). Sedimentation of algal organic matter consequently removes ^{12}C from surface-water DIC reservoirs. Increased productivity therefore is likely to yield an increase in the $\delta^{13}C$ of organic matter that is produced within the lake and becomes buried in its sediment.

The evolution of DIC and $\delta^{13}C_{DIC}$ begins with atmospheric CO_2 that has a $\delta^{13}C$ of about -7‰. Photosynthetic uptake of $CO_{2(atm)}$ is accompanied by significant depletion in ^{13}C (Clark and Fritz, 1997). The depletion occurs during CO_2 diffusion into the leaf stomata and dissolution in the cell sap, and during carbon fixation by the leaf's chloroplast, where CO_2 is converted to carbohydrate (CH_2O). The combination of these fractionating steps results in ^{13}C depletion in plant tissues. The amount of fractionation depends on the type of pathway used for fixation of organic matter. Plants use three principal photosynthetic pathways: the Calvin (C_3) cycle, the Hatch-Slack (C_4) cycle and the Crassulacean acid metabolism (CAM) (Clark and Fritz, 1997).

In the C_3 cycle, the first step is the fixation of CO_2 by the Rubisco enzyme, which catalyses CO_2 respiration through reaction with oxygen. The diffusion and dissolution of CO_2 has a net enrichment in ^{13}C. The C_3 plants dominate in cool, wet environments. Organic carbon that comes from C_3 plants is relatively very light and ranges between -24‰ and -30‰ (Clark and Fritz, 1997).

The $\delta^{13}C$ values of organic carbon that represent C_4 plants ranges from -10‰ to -16‰. C_4 plants dominate in hot open ecosystems such as tropical and temperate grasslands (Clark and Fritz, 1997). The PEP carboxylase enzyme act to deliver more carbon to Rubisco for fixation and the result is a reduction in ^{13}C fractionation during carboxylation.

CAM photosynthesis is favoured by 10% of the plant species. They have the ability to switch from C_3 photosynthesis during the day to C_4 pathway for fixing CO_2 during the night (Clark and Fritz, 1997). The $\delta^{13}C$ composition can be the full range of both C_3 and C_4 plants, but usually it is intermediate (Clark and Fritz, 1997). Alterations between C_3 and C_4 watershed plants accompany climate changes such as glacial/ interglacial transitions and wet/dry cycles, and these changes in land-plant types are evident in ^{13}C values of sedimentary organic matter (Meyers and Verges, 1999).

2.4 Description of Study Site

The study site is located in Northwestern Botswana. The site is part of an endorheic basin that drains a large watershed of approximately 530 000 km^2 (Ellery et al., 2003) located in the tropical Angolan highlands (McCarthy and Ellery, 1998) (Figure 1). The Okavango River originates in Angola, runs South East forming the border between Angola and Namibia, and finally enters Botswana. After 1600 km the river ends up in the Kalahari Desert, forming the Okavango Delta (Kranz and Vorwerk, 2007). The Makgadikgadi Pans are located south of the Okavango Delta and are connected by the Boteti River. The middle Kalahari comprises a vast internally drained basin in which aeolian, fluvial and lacustrine sediments have been accumulating since the Cretaceous times (Grove, 1969). Shorelines that have been mapped as remnants of a formerly extensive megapaleolake that linked the now discrete basins of Lake Ngami, Mababe Depression and Makgadikgadi Pans with the Okavango Delta to the north and the Kwando-Chobe-Linyanti rivers systems to the northeast are evidence of continuous body of water (Burrough et al., 2009).

The present-day Okavango River delivers its water and sediment load onto an alluvial fan (Okavango Delta) and partially into Lake Ngami and Makgadikgadi Pans that are now the terminus and natural sinks of endorheic sedimentation. The surface area of the alluvial fan is less than 10% of the entire river basin, thus given a discharge of approximately $1x10^9$ cubic metres per year brought into the Okavango Delta, the river therefore delivers potentially significant amounts of sediments into the basins. Based on old shorelines, two megalake systems have been identified (Shaw, 1988): an earlier and more expansive megapaleolake Makgadikgadi represented by shoreline features that occur at 940-945 m.a.s.l around the Lake Ngami, Mababe Depression and Makgadikgadi Pans (Shaw, 1988). The younger and less extensive palaeolake Thamalakane defined by shoreline features at 936 m.a.s.l seen along discrete shorelines around Lake Ngami and the Mababe Depression (Shaw, 1988) is understood to be contraction of the Paleolake Makgadikgadi.

Lower and unnamed paleolake levels were also recognised in the Makgadikgadi Pans at 920 m.a.s.l and 912 m.a.s.l, below which the water body broke up to form smaller separate bodies each of which functioned independently in terms of lower and younger stages of paleolake levels (McFarlane and Eckardt, 2006).

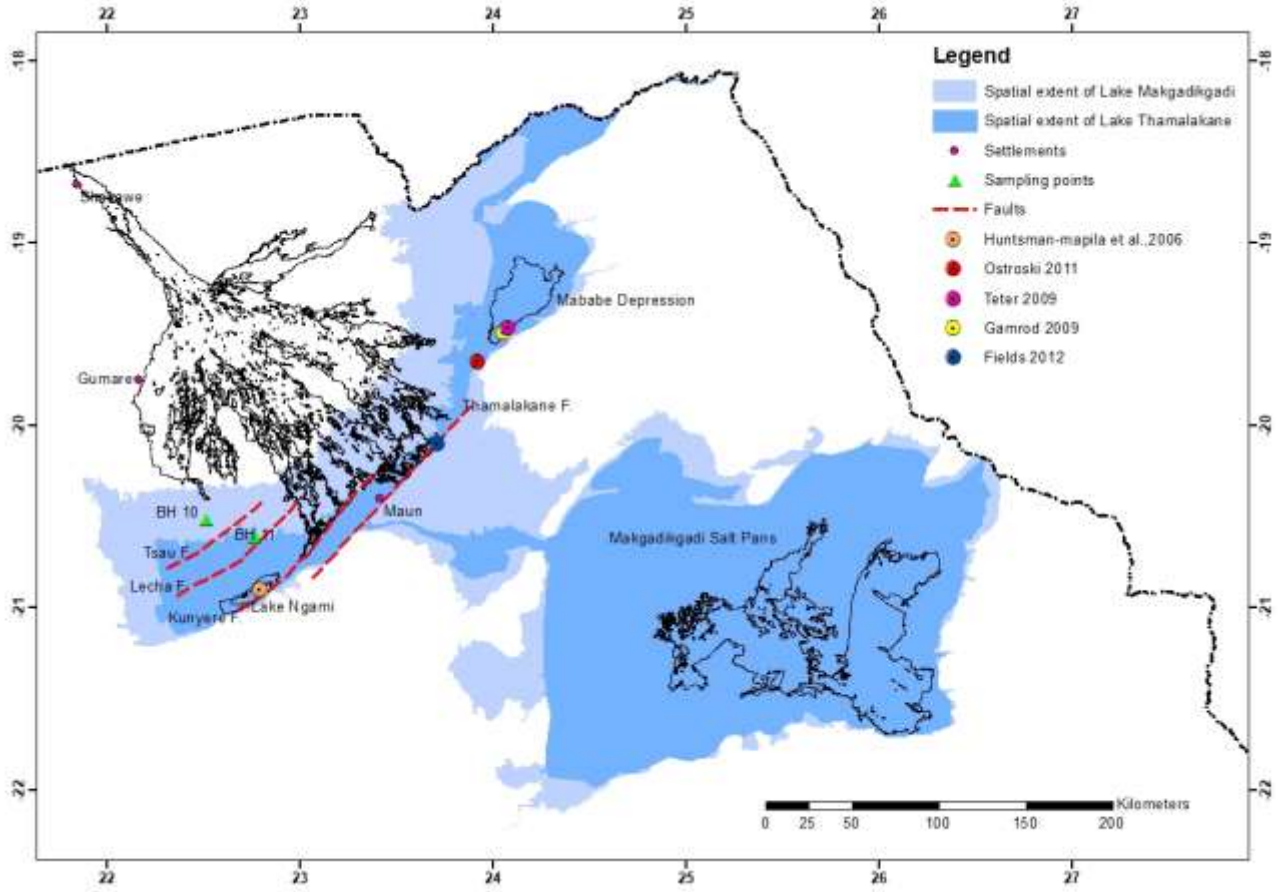

Figure 2**:** Physiographic locations of the sediments cores BH 10 and BH 11 relative to the projected extent of the middle-Kalahari megapaleolakes Makgadikgadi and Thamalakane (drawn using ArcGIS 10.4 with shapefiles from Botswana Department of surveys and mapping)

2.4.1 Geological and Tectonic Context of Northern Botswana

The surface geology around the Okavango Rift Zone (ORZ) primarily consists of unconsolidated Quaternary sediments that are restricted to the ORZ basin, the Quaternary Kalahari alluvium and Holocene lacustrine deposits within paleolakes (Cooke, 1984; Thomas and Shaw, 1991; Ringrose et al., 2005). The Quaternary unconsolidated sediments of the ORZ are underlain by lacustrine and fluvio-deltaic sediments of varying thickness. Bedrock, which is predominantly Precambrian crystalline rocks of the Damara and Ghanzi-Chobe orogenic belt are exposed to the northwest and southeast of the southwestern end of the ORZ (Bufford et al., 2012). The ORZ forms part of a north-easterly-elongated depression known as the Makgadikgadi–Okavango–Zambezi basin with a mean elevation of 850 m.a.s.l (Bufford et al., 2012). The basin is dominated by the south-easterly flowing drainage

system of the Okavango Delta, and the Kwando and the Zambezi Rivers. The ORZ consists of three depocenters represented by Lake Ngami sub-basin in the southwest, the Mababe Depression and the Linyanti-Chobe sub-basins to the northeast (Figure 1). The Ngami sub-basin represents a graben bounded by the NE-trending Kunyere Fault in the southeast and the Tsau Fault to the northwest. Similarly, the Mababe sub-basin is bounded in the northwest and southeast by the Tsau and the Mababe Faults, respectively (Figure 2).

2.4.2 Paleolake Basins and Climate Context of Northern Botswana

The climate of the middle Kalahari is semiarid with a mean annual temperature of 27.5 °C and a mean annual rainfall averaging 490 mm per year (Gumbricht et al., 2004). Local precipitation occurs mainly between October and February and is derived from convective scattered thunderstorms, the intensity of which is influenced by the position and strength of the Intertropical Convergence Zone (ITCZ) (Gumbricht et al., 2004). Both the climate and annual rainfall average are not enough to justify or maintain the size of the large paleolakes of the northern Kalahari.

The Makgadikgadi Pans are a series of dry and isolated lacustrine basins scattered over a large area and represent remnants of a formerly extensive lake system that formed large stable water bodies during the Quaternary (Moore et al., 2012). Periodically these basins would fill up to a point of coalescence (Burrough and Thomas, 2007) and inundate an area of approximately 66 000 km^2 to form the megapaleolake Makgadikgadi (MPL). Quaternary wet phases for the MPL have been dated at various timelines ranging from 131 ka down to 8.5 ka (Burrough et al., 2009) to infer the extent of basin’s water body.

CHAPTER 3

3.0 Methods

3.1 Samples Localities

Borehole samples were collected at two different localities as shown in Figure 2. The boreholes are located within the presumed boundaries of the MPL. The sites are named BH 10 (**S**20.0981 **E**22.52408) and BH 11 (**S**20.1865 **E**22.77033). These boreholes are located on the hanging wall side of the terminal faults, i.e. within the tectonic graben (Delta).

3.2 Field Investigation

Samples were collected from the lower end of the Okavango Delta at two distinct positions named BH10 and BH11 (see Figure 1). Sediments were collected as drill chips using reverse circulation rotary drilling at a sampling interval 1 m to a depth of 30 m below ground. The sediments were stored in ziploc bags and later analysed for various physical and geochemical properties of interest.

3.3 Laboratory Analyses

Aliquot of sediments were transferred from a ziploc bag into 25 mL glass scintillation vial. The lid of the vial was removed and the sample dried at 60^0 C in the glass vial for 72 hours.

3.3.1 Munsell Color Description

The color of the sediment was described using the Munsell color chart. The Munsell color (hue & value/chroma) was recorded. The colors were taken on dry samples.

3.3.2 Particle Sizes Analysis

Particle size analysis was performed using laser defractometry on a Cilas1180 particle size analyzer with a detection range of 0.04 to 2500 µm (Sperazza et al., 2004). Approximately 10 g of dried sediment was weighed and placed in 15 mL plastic centrifuge tubes. About 10 mL of 10% hydrochloric acid (HCl) was added to each centrifuge tube to digest carbonates. The tubes were sonicated for 15 minutes to disaggregate the sediments and then allowed to continue to react for 24 hours. The sediments were centrifuged for 5 minutes at 14,000 rpm for 10 minutes and the

supernatant was decanted. To ensure complete carbonate digestion, another 10 mL of hydrochloric acid was added again to each tube and allowed to react for 24 hours, centrifuged, and the supernatant was decanted. This was repeated until the samples no longer effervesced in contact with hydrochloric acid. Deionized water was added to each centrifuge tube, and the mixture centrifuged to remove residual hydrochloric acid. This step was repeated 3 or more times until the decanted liquid tested neutral on pH paper. At this point, approximately 10 mL of a 30% H_2O_2 was added to each sample and reacted for 24 hours to remove organic matter. Following this, the samples were centrifuged, the supernatant was decanted, and each sample was rinsed with deionized water 3 times until the pH tested neutral. The pre-treated sediments were individually added to 400 mL beakers and mixed with approximately 60 mL of 5% sodium hexa-metaphosphate $(NaPO_3)_6$ and allowed to sit for 12 hours. At the end of 12 hours, the samples were mixed using a magnetic stir bar for about 2 minutes before a 5 ml aliquot was introduced to the Cilas 1180 particle size analyzer by pipette. Samples were then measured 5 times, without ultrasonics, and analyzed using the Fraunhofer theory. Grain size distribution statistics were calculated according to the method of Folk and Ward (1957).

3.3.3 Magnetic Susceptibility

Magnetic Susceptibility values were measured on approximately 10 to 16 grams of samples on the basis of their mass (Ellwood et al., 2008). The high frequency magnetic susceptibility (X_{HF}) was measured for each sample using a Bartington MS2 magnetic susceptibility meter equipped with an MS2B dual frequency sensor. The X_{HF} is able to detect super fine grained minerals over the X_{LF}.

3.3.4 The Total inorganic Carbon (TIC)

The total inorganic carbon (TIC) concentration was determined by acidification under a vacuum and by extracting the CO_2 on a vacuum line using the technique of Krishnamurthy et al. (1997). The CO_2 concentration was determined manometrically and used to estimate the TIC concentration from a mass of the sample. The CO_2 was sealed in pyrex tubes for the determination of the stable carbon isotopes.

3.3.5 Stable Carbon Isotopes

Determinations of the isotopic compositions of organic carbon were made on decarbonated samples. The carbon elemental compositions were measured using a Costech ECS 4010 combustion elemental analyzer, coupled directly to a Thermo Finnigan Deltaplus XL mass spectrometer at Oklahoma State University, USA. The raw data were corrected for instrumental effects using the calibration curves obtained from the standards. Acetanilide concentration standards and graphite and USGS 40 were used for carbon isotope calibration. The $\delta^{13}C$ replicates for USGS 40 and graphite had standard deviations of $\pm$ 0.2‰. Standards were run after every ten samples to check for instrumental drift. For each sample run, four samples were run in duplicates and triplicates to estimate precision and accuracy. The CO_2 from the elemental analyzer and from TIS in the Pyrex tubes were analysed for the carbon isotopic composition using the Thermo Finnigan Deltaplus XL mass spectrometer. The Isotopic ratios are expressed in delta notation (δ) as per mil (‰) averages relative to standard using the following equation:

$$\delta\ (‰) = [R_{sample} / (R_{standard} - 1)] \times 1000$$

$$\text{where } R_{sample} = {}^{13}C/{}^{12}C_{sample} \qquad \text{(Hayes, 2004)}$$

$$R_{standard} = {}^{13}C/{}^{12}C_{standard}$$

The $\delta^{13}C$ values are reported relative to Vienna Pee Dee Belemnite (VPDB).

CHAPTER 4

4.0 Results

Analyses of sediments physical properties (grain size distribution, munsell colour and magnetic susceptibility) and chemical properties (TIC, TOC and $\delta^{13}C$) are presented in graphics in Figures 3 and 4). Results are presented in Appendices A to C. Three (3) major stratigraphic units delineated over the 30 meter core length for borehole 10. Borehole 11 has 2 units that are further divided into sub-units based on frequency of interbedding between sand rich and clay/silt rich layers and other indicators (X_{hf}, TIC, TOC and $\delta^{13}C$).

4.1 BH 10

Sediments for BH 10 are shown in Figure 3 and consist of 3 units: BH10-I at the base, BH 10-II in the mid-section and BH 10-III at the top.

4.1.1 BH 10: Unit I

BH 10-I is 2 m thick and extends from 916 m a.s.l to 918 m a.s.l. It is light brownish gray in colour (2.5Y 6/2). The bottom of the unit is 75% sand, 19% silt and 6% clay. The top of the unit is 91% sand, 7% silt and 2% clay. Magnetic susceptibility (X_{hf}) values decrease from $1.7x10^{-8}$ m^3/kg at the bottom of the layer to $1.47x10^{-8}$ m^3/kg at the top of the layer. The TIC and TOC concentrations are invariant at around 0.05%, and the carbon isotopic composition ($\delta^{13}C$) values averages -26.2‰.

4.1.2 BH 10: Unit II

This unit is 22 m thick extending between elevations 918 m a.s.l to 939 m a.s.l. The unit is light brownish gray (2.5Y 6/2) at the base, pale yellow (2.5Y 7/3) in the mid-section and light gray (2.5Y 7/2) at the top. Grain sizes consists of sand (89%), silt (9%) and clay (2%). All other proxy indicators ($X_{hf,}$ TIC, TOC and $\delta^{13}C$) are non-responsive throughout the layer. X_{hf} is at an average of $0.6x10^{-8}$ m^3/kg, TIC constant at 0.05%, TOC at 0.05% and $\delta^{13}C$ averages at -26.0‰.

4.1.3 BH 10: Unit III

The youngest unit for BH 10 is 6 m of sediment extending from 939 m a.s.l to 945 m a.s.l. The sediment colour is light gray (2.5Y 7/1) at the bottom to very dark gray

(10YR 3/1) at the top of the unit. The unit progresses from being dominated by sand at the bottom to towards silts and clays towards the surface. On average sand is 41% while the silt plus clay make up 59%. The X_{hf} values show a progressive increase from $0.4x10^{-8}$ m^3/kg at the base of the unit to $2.0x10^{-8}$ m^3/kg at the top (surface). The TIC is invariable from base to the surface at 0.1% with a small positive spike in the data around 942 m a.s.l. TOC shows progressive increase in organic carbon from 0.05% at the base to about 0.5% at the top (surface). The $\delta^{13}C$ values gradually increase from -26.7‰ at the base towards -19.6‰ at the surface, with an average of -23.6‰ for this unit.

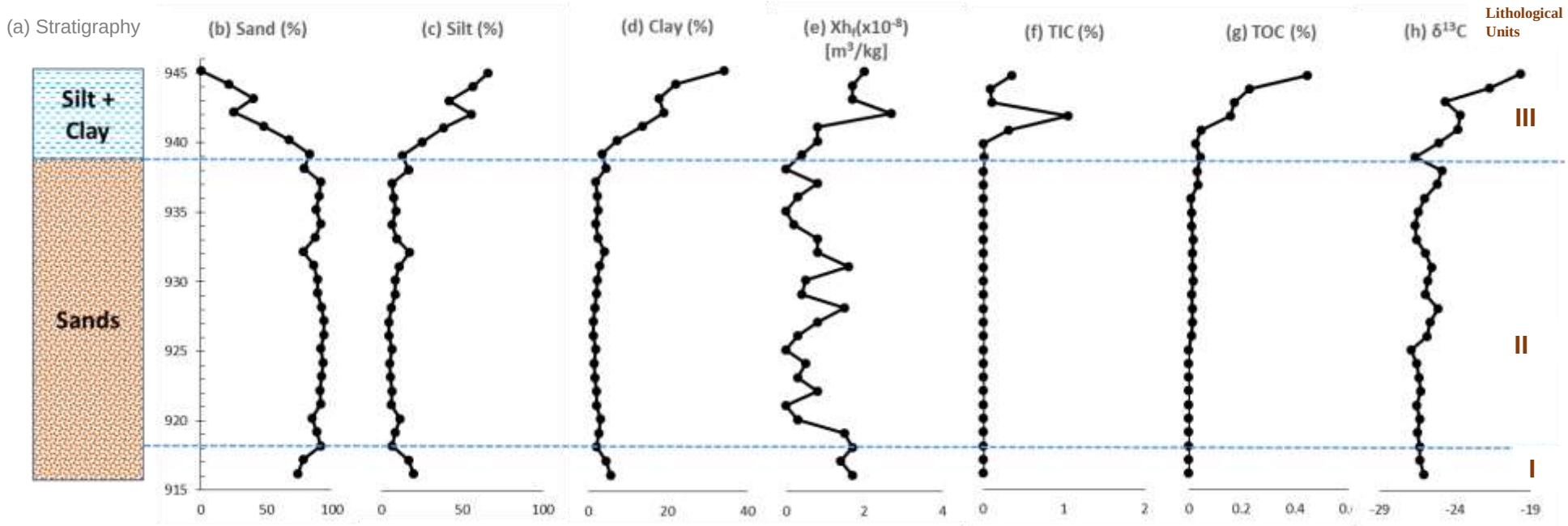

Figure 3:(a) Borehole stratigraphy (b) Percent sands (c) Percent silt (d) Percent clay (e) High frequency magnetic susceptibility (X_{hf}) (f) Percent TIC (g) Percent TOC (h) Stable carbon isotopic ratios of TOC for site BH 10

4.2 BH 11

Sediments for BH 11 are displayed in Figure 4 and consist of 2 major intervals: BH11-I at the base and BH 10-II at the top with 8 sub-units.

4.2.1 BH 11: Unit I

The oldest unit is 4 m thick ranging between elevations 911 m a.s.l and 914 m a.s.l. The unit is light brownish gray (2.5Y 6/2) at the bottom to pale brown (2.5Y 8/2) at the top. The unit has a high percentage of sand grains (86%), silt (11%) and clay (3%). X_{hf} values for this unit range from about $1.1x10^{-8}$ m^3/kg at the base of the unit and decrease to $0.8x10^{-8}$ m^3/kg at the top of the unit. The TIC is invariant at 0.05% while the TOC concentrations decrease from 0.05% at the base to 0.01% at the top of the unit. The $\delta^{13}C$ values averages -26.5‰.

4.2.2 BH 11: Unit II

This unit is made up of several interlayered beds of silty clays and sandy silts. It consists of 4 beds of sandy silts and 4 layers of silty clays, (8) sub-units in total (II-1, II-2, II-3, II-4, II-5, II-6, II-7 and II-8) to represent the variation in sediments facies from bottom to top across the unit. The sediments thickness for this layer is 26 m total.

4.2.2.1 BH 11: Unit II-1

This unit is 7 m thick (914 m a.s.l-921 m a.s.l) and is pale brown (10YR 8/3) in colour entirely. The unit has an increase in fines from bottom to top of the unit. At the bottom of the unit, the unit has silt (50%), sand (40%) and clay (10%), while at the top it has about silt (70%) sand (10%), and clay (20%). Drastic grain sizes change from sand to silt+ clays (predominantly). The X_{hf} values increase from $0.8x10^{-8}$ m^3/kg at the base to $1.7x10^{-8}$ m^3/kg at the top of the unit. The TIC concentration is close to 0.01% and increase slightly at the top of the unit to 0.05%. TOC is steady at 0.01% during the first half of the layer and begins to increase towards the top at 0.05%. The $\delta^{13}C$ values averages -27.2‰.

4.2.2.2 BH 11: Unit II-2

This is 3 m thick (921 m a.s.l-924 m a.s.l) and is pale brown (10YR 6/3) at the bottom of the unit to very pale brown (10YR 7/3) at the top. It is mainly sand (66%) with less proportions

of silt (27%) and clay (7%). The X_{hf} values for this unit are $1.7x10^{-8}$ m^3/kg at the bottom and $0.8x10^{-8}$ m^3/kg at the top. TIC and TOC are consistent at 0.05% each. The $\delta^{13}C$ values averages -26.3‰.

4.2.2.3 BH 11: Unit II-3

BH 11-II-3 is 1 m thick ranging between 924 m a.s.l and 925 m a.s.l and is very pale brown (10YR 7/3). It has a high proportion of silt (46%) and clay (16%), and less sand (38%) making it more clayey than sandy. The X_{hf} values increase from $0.9x10^{-8}m^3/kg$ at the bottom to a high of $2.1x10^{-8}m^3/kg$ at the top. TIC concentration is at about 0.18% and TOC is around 0.06%. The $\delta^{13}C$ values averages -25.6‰.

4.2.2.4 BH 11: Unit II-4

This layer is 5 m thick and extends from 925 m a.s.l to 930 m a.s.l and is very pale brown (10YR 7/3). The unit has high sand content (66%) and lesser proportions of silt (27%) and clay (7%), hence mapped as a sand layer. The X_{hf} values decrease from base ($0.8x10^{-8}m^3/kg$) to top ($0.5\ x10^{-8}m^3/kg$). TIC concentration increases in the lower 3m (0.12%) and drops in the top 2m of the layer (0.07%). TOC concentration show slight increase from base (0.03%) to the top of the unit (0.04%). The $\delta^{13}C$ values averages -25.9‰.

4.2.2.5 BH 11: Unit II-5

Sub-unit BH 11-II-5 is a 1 m thick layer extending from 930 m a.s.l to 931 m a.s.l and is very pale brown (10YR 7/3). It consists of (60%) fines (silt 47% and clay 13%) and sands at 40%. It is mapped as clay silt. The X_{hf} values are increasing from the bottom of the unit ($0.5x10^{-8}m^3/kg$) to the top ($4.1x10^{-8}m^3/kg$). TIC concentration is at 0.05% and TOC concentration decreases from the base of the unit at 0.05% to the top at 0%. The $\delta^{13}C$ value is -25.4‰.

4.2.2.6 BH 11: Unit II-6

This layer is 5 m thick, extending from 931 m a.s.l to 936 m a.s.l and it is very pale brown in colour (10YR 7/3). The content of sand is 66%, silt is 27% and clay is 7%. Hence the layer is mapped as a sand layer. The X_{hf} values are increasing ($3.4x10^{-8}$ m^3/kg to $7.7x10^{-8}$ m^3/kg) at the bottom and decrease to the top of the unit ($0.3x10^{-8}m^3/kg$). TIC is lower at the base

(0.05%), peaks at the middle section (0.12%) and drops towards the top of the unit (0.07%). The TOC concentration increases from the base of the unit (0.03%) to the top of the unit (0.04%). The $\delta^{13}C$ values averages -24.7‰.

4.2.2.7 BH 11: Unit II-7

BH 11: Unit II-7 is a 1 m thick and extends from 936 m a.s.l to 937 m a.s.l. The sediments are is pale brown in colour (10YR 6/3). They have a sand content of 20% and a higher contents of fines (silt 64% and clay 16%).The X_{hf} values increase from the base ($0.3x10^{-8}$ m^3/kg) to the top ($1.6 x10^{-8}$ m^3/kg) of the unit. The TIC content is 0.13% and TOC invariable at 0.05%. The isotopic composition of organic matter shows an increase from -25.0‰ at the bottom to -23.2‰ at the top.

4.2.2.8 BH 11: Unit II-8

This unit extends for 3 m from an elevation of 937 m a.s.l to 940 m a.s.l. The sediments are pale brown (10YR 6/3) to brown (7.5YR 5/2) in colour and are made up of a mix of sand (59%), silt (32%) and clay (9%). The X_{hf} values are increasing from the bottom ($0.8x10^{-8}$ m^3/kg) to the middle section of the unit ($1.3x10^{-8}$ m^3/kg) and decreases to the top ($1.1x10^{-8}$ m^3/kg). The TIC values decrease from 0.07% at the base to 0.05% at the top of the unit. TOC values range around 0.05% while $\delta^{13}C$ show an isotopic increase from -23.2‰ at the base to -20.6‰ at the top of the unit.

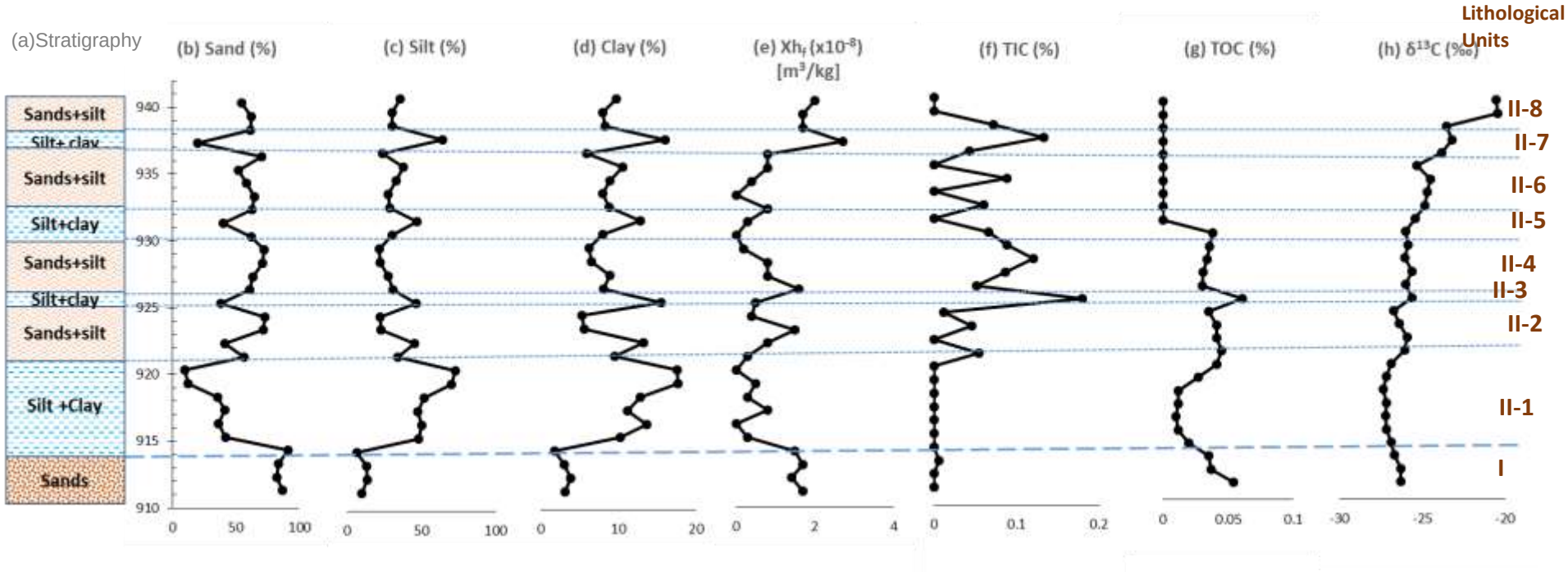

Figure 4: (a) Borehole stratigraphy (b) Percent sands (c) Percent silt (d) Percent clay (e) High frequency magnetic susceptibility (X_{hf}) (f) Percent TIC (g) Percent TOC (h) Stable carbon isotopic ratios of TOC for site BH 11

CHAPTER 5

5.0 Discussion

Grain size analysis of sediments within the lake basin is the primary tool used to delineate whether or not sediments being deposited are of local or distal origin. Local sediments supplied by channels as well as from nearby dune fields and beach ridges, for instance, will have a larger average grain size and higher sand content than sediments originating from distal sources such as the Angolan highlands. Sediments from Angolan highlands are altered by the fractionating effects of the Okavango Delta swamp and, therefore, will contain higher percentages of silt and clay-sized material, and little, if any, sand-sized sediment. Additionally, the lithology of the sediment section and the thickness of each of the lithologies can be used to distinguish periods dominated by local and regional sedimentation. The influence of a local climate would result in the occurrence of sand-sized sediments and the appearance of lithologies such as sandy-clay silts, whereas the effects of a regional climate would be manifest in the lake record as clay.

5.1 Site BH 10

5.1.1 Physical Properties of sediments and climatic units

The core is made up of a succession that is sand rich at the bottom and silt and clay rich at the top. The heterogeneity in the sediment succession is indicative of a changing depositional environment or a changing sediment source therefore can be interpreted as a paleoclimate proxy.

The two units in Figure 5 are possibly derived from two different sources. The lower sandy unit represents materials that have lower MS. The interpretation offered for this scenario is that the sandy unit was deposited from erosion of the local sand dunes that are magnetically poor. The upper 7 m of the core is a unit that is rich in clay, progressively getting poorer in the sand content towards the top and a higher MS. This shows sediments characteristics that are contrasting for both units, possibly indicating a change in the sediment source. For the upper unit here is evidence of changing source provided by abundant clayey material and increased MS values.

The local Kalahari landscape is not rich in rocks of high magnetic concentrations (Bufford et al., 2012) therefore source of the sandy unit could be inferred to be the

local landscape. Most of the coarse grained sediments like sand that come with the Okavango River inflow get filtered out in the panhandle area therefore not likely to reach the downstream areas of the middle Kalahari (McCarthy, 2013). Conversely, the clay-rich unit is likely derived from a different terrane that has rocks of higher magnetic properties. Such rocks as granitoids, gabbros and related volcanic rocks are found in catchment of the Okavango River in the sub-tropical areas of Angola (Huntsman-Mapila et al., 2006).

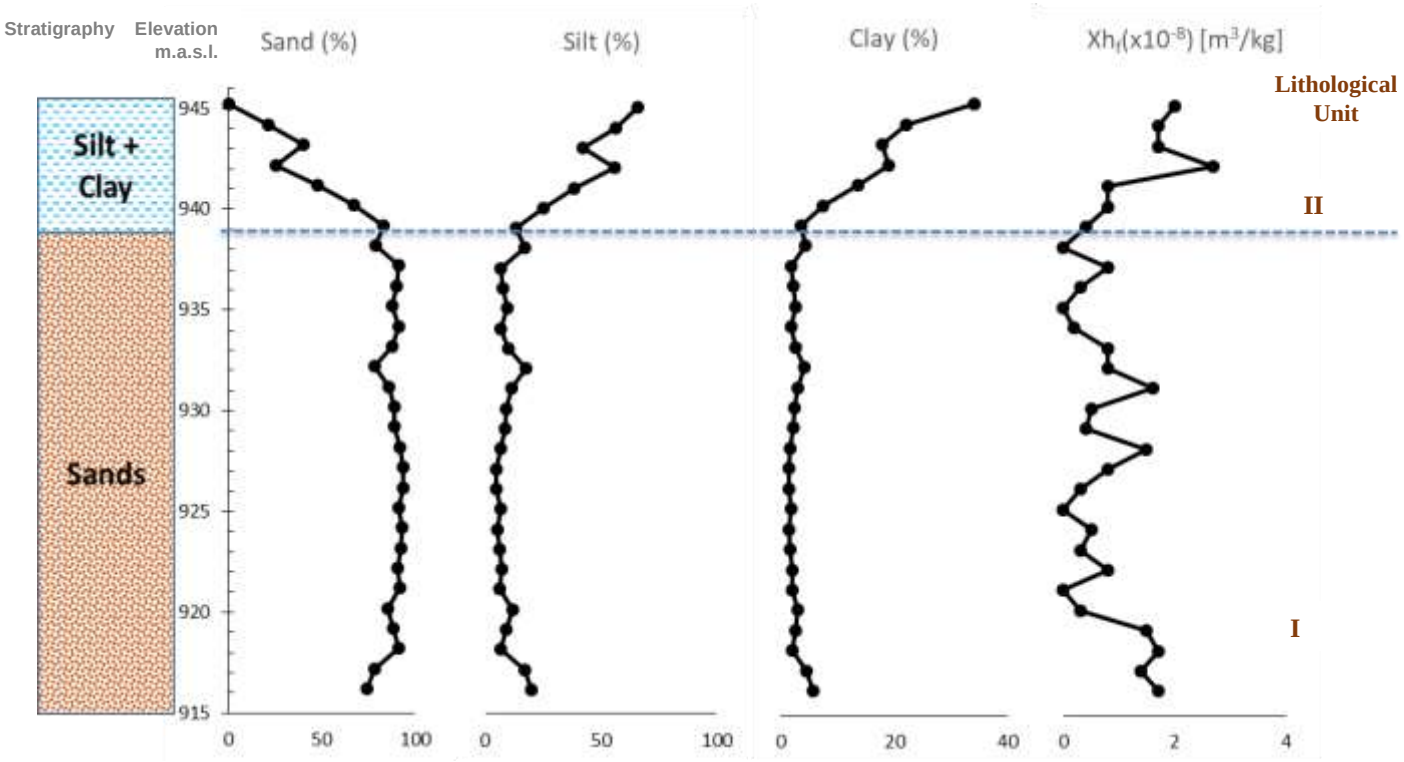

Figure 5: Borehole stratigraphy, grain sizes analyses and magnetic susceptibility of sediments with interpreted hydrodynamic conditions and sediment provenance for BH 10

5.1.2 Chemical and Isotopic properties of sediments and climate variability

Using the chemical and isotopic variations along the length of the core as proxies the core was divided into two major phases of climate, namely Phase I and Phase II.

5.1.2.1 Phase I (914 m a.s.l - 939 m a.s.l)

Phase I is characterised by relatively low content of both TOC and TIC from the bottom to the 939 m a.s.l elevation. There is low content of organic matter (TOC), from the bottom until 939 m a.s.l. The areas of low TOC are also isotopically depleted. The interpretation offered for this scenario is that the sandy unit was deposited when the local climate was wet, and with little or no contribution from any external sources. Low

TOC concentration within the sandy unit is evident of limited vegetation cover, hence the local environment wet as it could have been, was also deficient in plant material.

5.1.2.2 Phase II (939 m a.s.l - 945 m a.s.l)

Between 939 m a.s.l and the surface all the three properties (TOC, TIC and $\delta^{13}C$) show major changes as shown in Figure 6. The TOC concentrations drastically increase from their lowest and constantly increase until the surface. The high concentrations may relate to the increased input of vegetation. The increased TOC concentration and organic matter that is isotopically heavier than in Phase I. The TOC shows increased plant activity which is un-characteristic of the local sediment source. The $\delta^{13}C$ suggests that the vegetation is derived from a landscape that was different i.e. -20‰ indicative of less wet conditions. The $\delta^{13}C$ progressively moves away from conditions of wet (-26 ‰) at the boundary towards dry, and suggests that the landscape where the material could have been derived from a relatively drier landscape (~ -14‰). The isotopic signature shows progressive enrichment which could also be a dilution effect between locally derived material and material from regional source. The change in the vegetation type is significant for this portion and can be interpreted as evidence for a changing regional climate.

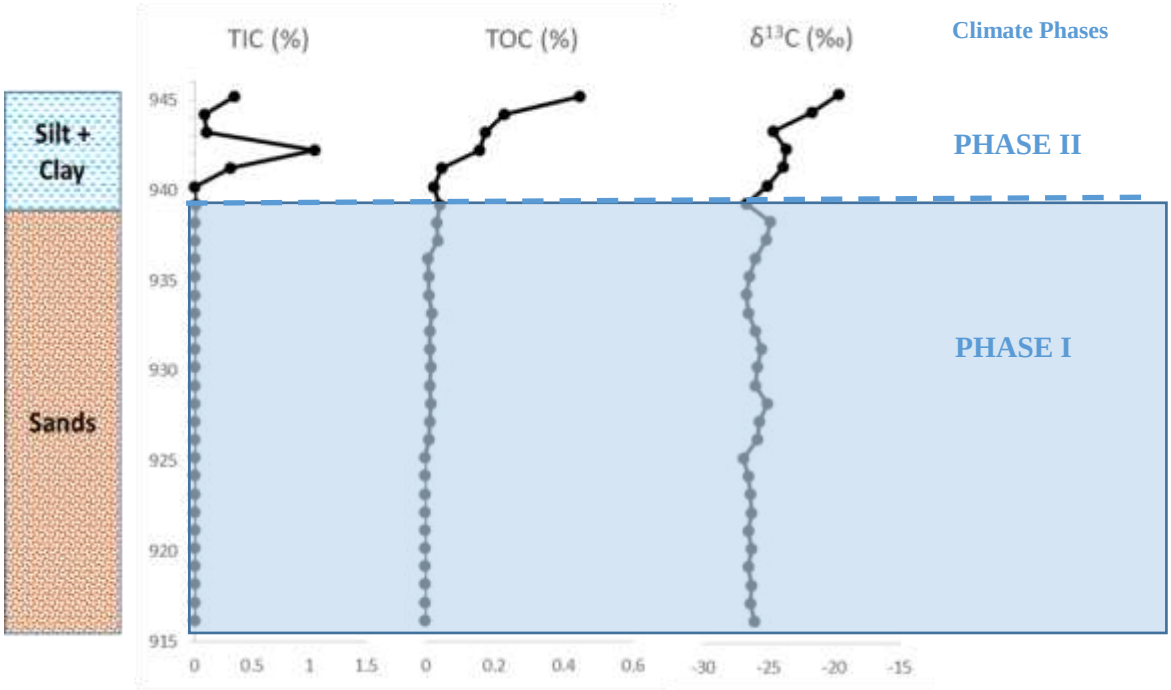

Figure 6: Borehole stratigraphy, TIC concentrations, TOC concentrations and organic matter $\delta^{13}C$ of sediments with interpreted climate model for site for BH 10.

The light blue solid colour represents the interval during which lacustrine sedimentation occurred.

5.2 Site BH 11

5.2.1 Physical properties of sediments and climatic units

Sediments characteristics are useful in reconstructing hydrological conditions, sediments provenances and variations in past climates (MacDonald et al., 2000). The core is made up of a succession of predominantly sand-rich beds that are periodically interlayered with beds that are rich in silt and clay. This periodic succession of facies between sand-rich and silt/clay-rich units is indicative of a changing depositional environment and therefore can be interpreted as a paleoclimate proxy. In general, Figure 7 shows that the units that are rich in silt and clay correspond with magnetic susceptibility positive peaks as opposed to ones that have a higher content of sand. This interlayered succession may infer a sediment source that is changing over the depth of the core.

According to Huntsman-Mapila et al., 2006 lakes of the middle Kalahari in northern Botswana receive water and in part sediments from the sub-tropical Angolan watershed through the Okavango River. The sediments characteristically have high magnetic properties as they are derived from that are rich in volcanic rocks. On the contrary, the local watershed is dominated by sand dunes (Ringrose et al., 1999) that are poor in magnetic minerals and therefore relatively inferior in their magnetic properties. As a result, the sand-rich beds are interpreted as derivatives of the eroded sand dune landscape of the Kalahari environment (e.g. Burrough et al., 2009) whereas the silt/clay-rich beds are fluvial deposits that are derived from the external sub-tropical source. The fact that the sands come from a local sand-rich source may suggest that they are products of aeolian processes, and likely representing a drier environment.

The sand/silt-clay succession may therefore be used to assess paleo-environmental conditions when climate transitioned between relatively drier and wetter episodes. The deposits are probably related to the dynamics of the Okavango-Chobe-Linyanti Rivers that flowed into the Makgadikgadi during the Quaternary (Jones, 1980; Thomas and Shaw 1991). Burrough and Thomas (2008) also noted that paleolakes observed in the Kalahari region suggest a significant and increased flow in the Chobe-Zambezi system that contributed to the middle Kalahari lake phases. The heterogeneity in the

sedimentary facies of Figure 7 therefore may be indicative of a changing sediment source area and varying depositional environment.

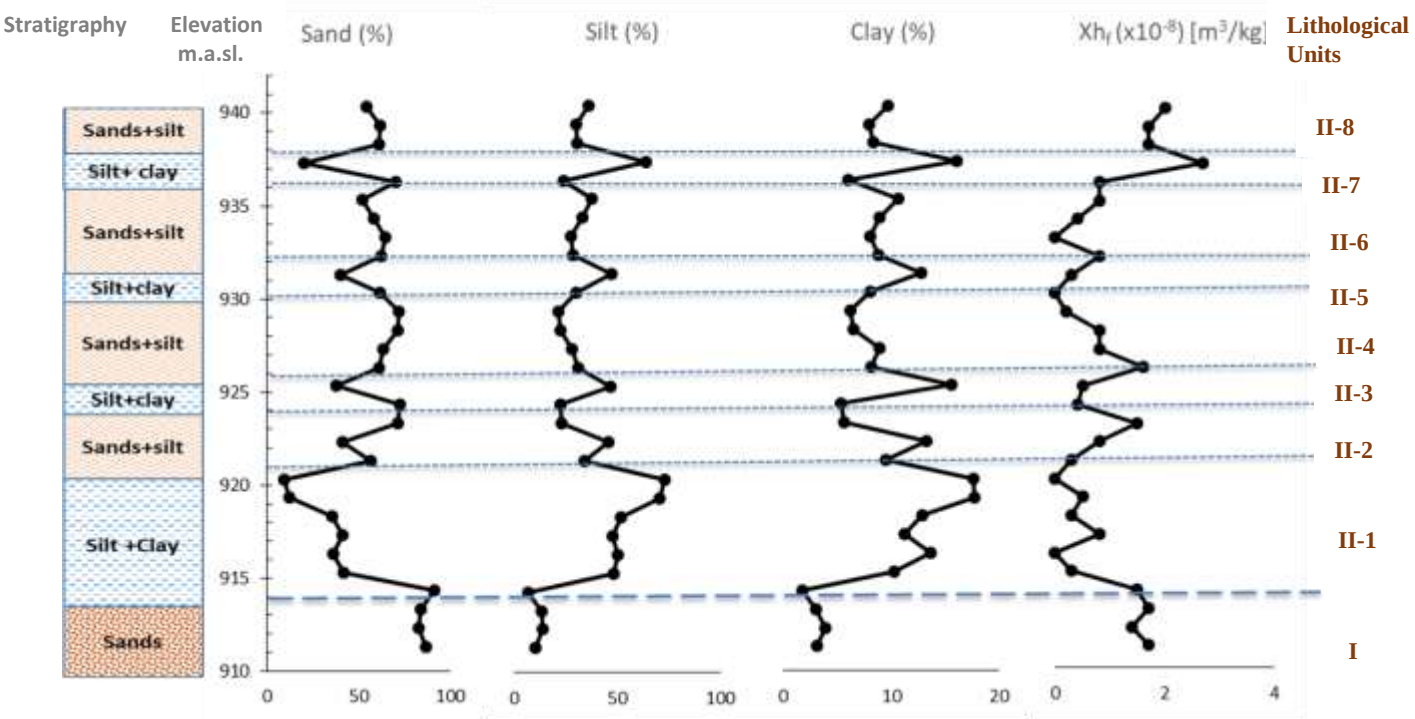

Figure 7: Borehole stratigraphy, grain sizes analyses and magnetic susceptibility of sediments with interpreted hydrodynamic conditions and sediment provenance for BH 11

5.2.2 Chemical and isotopic properties of sediments and climate variability

Using the chemical and isotopic variations along the length of the core as proxies, the core was divided into two major phases of climate, namely Phase I and Phase II.

5.2.2.1 Phase I (911 m a.s.l to 934 m a.s.l)

The lower portion of the graph (910-913 m a.s.l.) in Figure 8 is characterised by a little decreasing organic matter (TOC) content going upwards Decreasing TOC likely indicates limited vegetation productivity (Meyers, 2003) that may be related to increasing moisture deficiency, hence suggesting a climate that was drying up. Corresponding to this are consistently low TIC concentrations suggesting that the conditions were not significantly arid to precipitate carbonate material in the sediments, except very close to the top of the unit where there is a small positive spike to indicate increasing aridity. The $\delta^{13}C$ of organic matter during this interval was constant showing no significant changes in vegetation type. The values remained

within the C_3 landscape, therefore signifying conditions of a cool and wet climate (Fritz and Clark 1997).

Major increases in the chemical concentrations were observed in the mid-section of the core from 913-932 m a.s.l. This is the section that shows a repetitive sequence of alternating clay-rich silts and predominantly sand-rich layers. Layers that are rich in clays correlate positively with increasing TOC concentrations. Higher TOC in the sediments would mean increased vegetation productivity (Meyers, 2003) or a more widespread vegetation cover (Burrough et al., 2009a). Clays are common deposits of deep water environment (McFarlane et al., 2005), therefore a correlation of high TOC and high clay content in the sediments may support a humid climate. The consequence of this humid period is therefore more obvious in terms of the cycling of carbon between plants and sediments. The section has a constant and low concentrations of TIC indicating that all carbonate minerals went into solution. This is common when there is high water content to dissolve minerals, hence supporting a climate that was more humid. The presence of more water and a larger vegetation cover and density must have enhanced weathering of organic matter and activated such elemental cycling with impacts on the chemical balances of TOC and TIC. The $\delta^{13}C$ of organic matter during this interval was shifting towards more negative values, i.e. less than -26‰ indicating increasing wetness.

Subsequent layers that rich in sand tend to be relatively poorer in TOC concentration. This point to a changing environment from widespread vegetation to a lesser vegetated one. The sandy layers also show several peaks of enriched TIC indicating that the layers could not have been deposited under conditions similar to the clay-rich layers. High TIC in the sediments shows there was chemical precipitation of carbonate material related to loss of water, and therefore a drying up environment. As indicated earlier, the silty sands are characteristic of sediments of the present-day Kalahari landscape (Ringrose, et al., 1999) and therefore likely to represent deposition under a dry environment.

Organic matter isotopic compositions ($\delta^{13}C$) sediments can be good indicators for mapping shifts in vegetation cover, hence changing environmental conditions (Leng and Marshall, 2004). The $\delta^{13}C$ values on this portion of the core fall within the C_3 landscape (~ -26‰) showing a wet and cool climate. The $\delta^{13}C$ values for this section

are relatively lighter, i.e. up to -28‰, indicating increasing water content, and correlate with layers that are rich in clay.

From the chemical properties of the sediments the presence of alternating clays and sands possibly indicate several phases of lake high stand interchanging with a dry lakebed respectively. These cycles of wet and dry climate did not impact the land vegetation that much. The vegetation cover for this unit does not change in type indicating that within the generally wet phase of climate there were several short-term episodes of aridity as shown by periodic and higher TIC concentrations.

5.2.2.3 Phase II (934 m a.s.l to 940 m a.s.l)

Between 934 m a.s.l. and the surface all the three properties (TOC, TIC and $\delta^{13}C$) show major changes. The TOC concentrations drastically fall to their lowest and remain low until the end of the core. The low concentrations may relate to the absence of a significant input of vegetation biomass during this interval. The interval also shows periodic and frequently fluctuating concentration of TIC that may signify repeated cycles of aridity. The $\delta^{13}C$ values shift from isotopically lighter values (~ -26‰) to heavier values (~ -20‰). The heavier values are possibly dilution between C_3 and C_4 vegetation, and reflect a diminishing delivery of organic matter of isotopically light C_3 plants towards enriched C_4 type. The change in the vegetation type is significant for this portion and can be interpreted as evidence for a changing climate. C_4 type vegetation is favoured in an environment of decreasing availability of water, hence a drier climate (O'Leary, 1988). The responses from the chemical and isotopic content of the sediments are particularly significant because they signify a major change in the environment from a cool wet climate with higher vegetation productivity and more water in the lake to a warmer and drier environment characterised by lower vegetation biomass, less water and frequent precipitation of carbonate material. The change marks the end of a major wet period, and probably the demise of a major fluvial system, and the emergence of a new and drier cycle in climate. The observed drier phase is likely similar to present-day settings of a warm and dry climate.

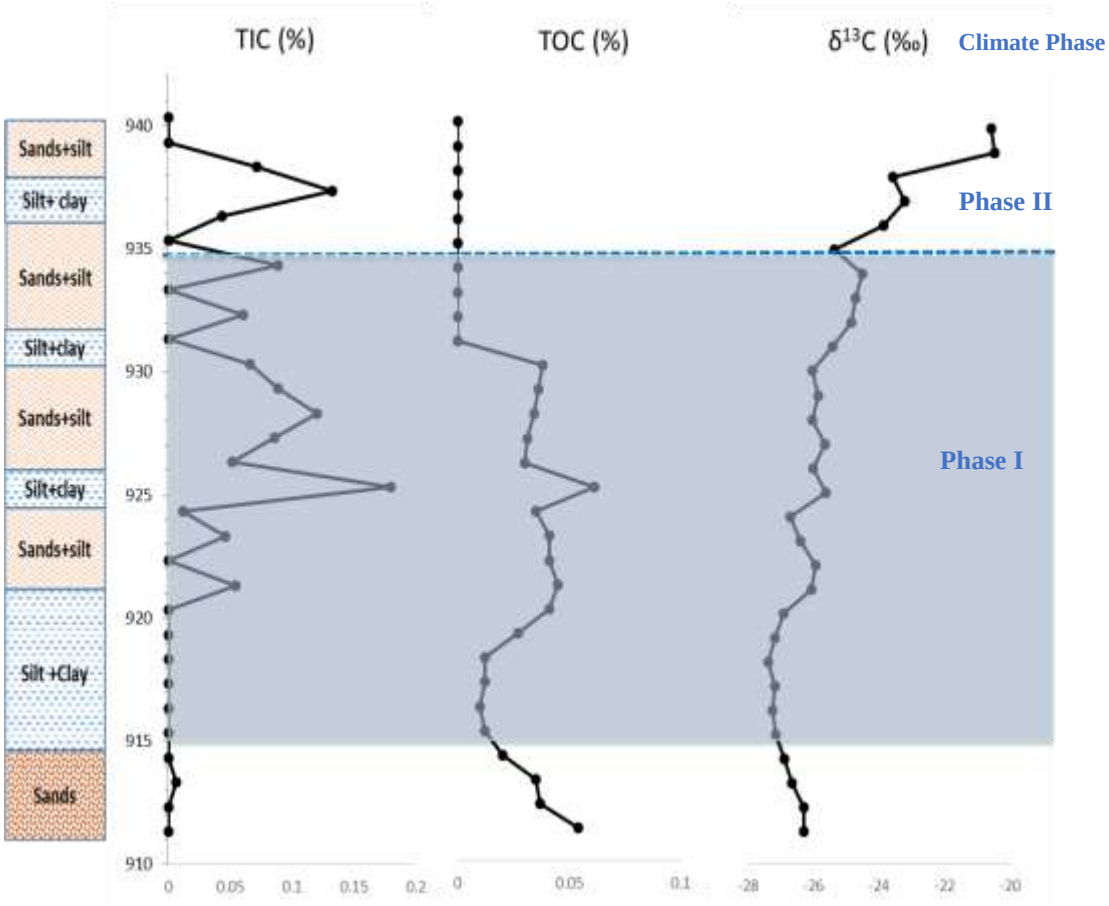

Figure 8: Borehole stratigraphy, TIC concentrations, TOC concentrations and organic matter $\delta^{13}C$ of sediments with interpreted climate model for site for BH 11.

The light blue solid colour represents the interval during which lacustrine sedimentation occurred.

5.3 Grain size distribution

The grain size distribution for lake sediments (Thomas, 1987; Shaw et al., 2003; Burrough et al., 2007; Fields, 2012; Ostroski, 2011) compared to the sediments from BH 10 and BH 11 is shown in Figure 9 and summarised in Table 1. The percent sand for BH 10 sediments is approximately 77% is more consistent with the 73% average sand content of the lake sediments from previous studies. The percent silt and clay for BH 10 sediments is approximately 17% and 6%, respectively, are also similar to those in lake sediments, which average 22% for silt and 5% for clay. The percent sand for BH 11 sediments ranges between 0.16% and 93% which is approximately 56% on average, it is consistent with the 73% average sand content of the lake sediments from previous studies. The percent silt and clay for the sediments is approximately 35% and 9%, respectively, are also similar to those in lake sediments, which average 22% for silt and 5% for clay. From comparable grain sizes characteristics with sediments

from previous studies of other lake sediments in the area we argue that the grain size distribution of the sediments from both BH 10 and BH 11 can be attributed to deposition in a lake setting.

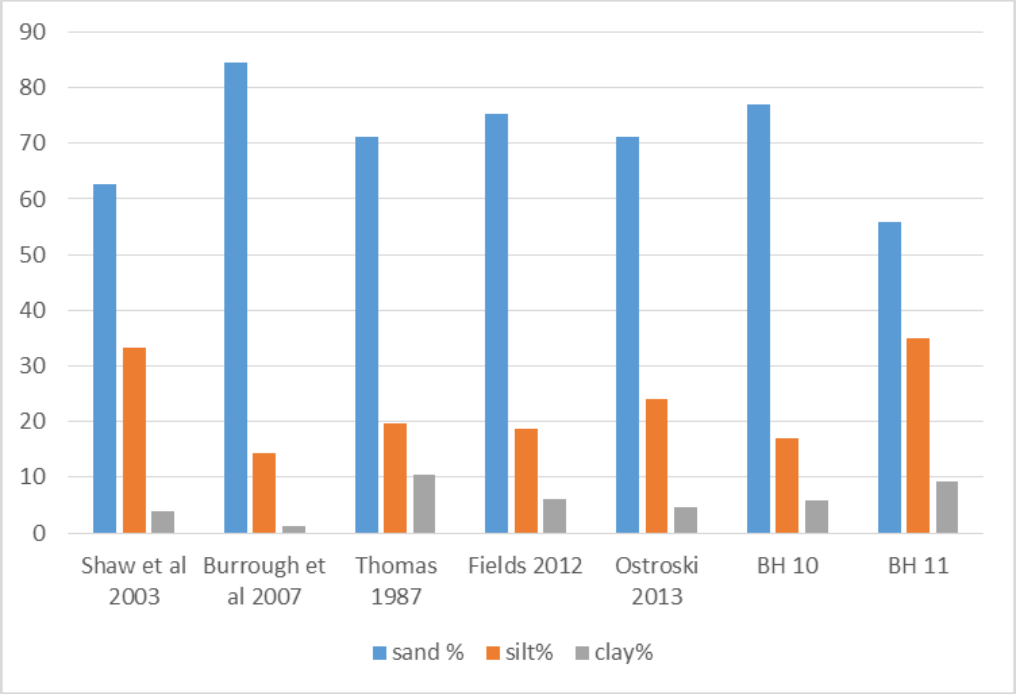

Figure 9: Lacustrine sediments from studies of other middle Kalahari areas compared to the sediments of the current study.

Table 1: Lacustrine sediments from studies of other middle Kalahari areas compared to the sediments of the current study.

	Shaw et al (2003)	Burrough et al (2007)	Thomas (1987)	Fields (2012)	Ostroski (2013)	**BH 10 Current Study**	**BH 11 Current Study**
Sand (%)	62.7	84.4	71.2	75.2	71.2	**77.1**	**55.8**
Silt (%)	33.3	14.4	19.6	18.6	24.1	**17**	**34.9**
Clay (%)	3.9	1.2	10.4	6.2	4.7	**5.9**	**9.3**

CHAPTER 6

6.0 Conclusions and Recommendations

6.1 Sedimentation and stratigraphic perspective and evidence of paleoenvironments

A critical observation of the two cores reveals two distinct episodes of sediments generations. The first 24 m of the core is made up by a thick layer of sand (BH 10) that possibly formed when favourably wet local condition that eroded the local Kalahari landscape. Sediments in the upper 7 m of the core are mainly clay and silt and that deposited in a drying up environment of a lacustrine nature. The silt and clay possibly were contributed by rivers that tapped from regional watersheds during times of favourably wet hydrologic conditions. As a result, two climate events have dominated the area since the Quaternary, being an earlier hydrologically wet period that filled up the lakes followed by a relatively drier one that evaporated them.

For BH 11, the lower 24 m of the core has several units of sand that interlayered with those of silt and clay. This indicates a changing sediments source and hydrologic input within a broader humid condition. As a result it may be postulated that climate in the lower portion, though generally humid, also underwent periodically short term oscillations between wet and dry because of interlayered nature of clay and silt with sands. Two sources of sediments into the paleolakes are identified. The first erosion of the proximal Kalahari watershed when local rivers from the south of the paleolakes delivered sands under locally more humid conditions. The other source is considered distal and delivered finer grained bedload sediments from the Okavango River to and other regional rivers from the north during hydrologically wet conditions (McCarthy and Ellery, 1998). Therefore, hydrologic input from the distal watershed in the Angolan highlands and from local watersheds in the middle Kalahari likely caused variations in the proportions and types of sediments delivered to the paleolakes.

6.2 Magnetic susceptibility

The magnetic susceptibility values of the sediments in the lower 24 m of both sediment cores followed no particular trend but only slightly fluctuated along the core length. After 24 m the measurements clearly increased to higher values that approach 2.0 x $10^{-8}m^3kg^{-1}$ which is still within normal range (< 10 x $10^{-8}m^3kg^{-1}$). Higher values in the upper 7 m of the cores associate closely with the clay/silt layers and could relate to

catchments with rocks are richer in magnetic minerals. The Kalahari environment is devoid of such rocks, therefore the next likely source with higher magnetic minerals concentrations would be the distal igneous terrains of the Angolan highlands (Huntsman-Mapila et al., 2005) that are is rich in granitoids, gabbros and related volcanic rocks. Lower concentrations associated with layers of sand would suggest that sediments are sourced from local catchments of the middle-Kalahari and around the Okavango Delta (Huntsman-Mapila et al., 2005). It is argued therefore that from the sediments with higher MS values come from a distal source that hosts rocks of higher magnetic minerals when regional hydrologic inputs were also higher. Lower MS in the sediments would mean they were sourced from a local landscape with lower concentrations of primary magnetic minerals.

6.3 Carbon Dynamics

All the carbon indicators show only one major break between the lower 24 m of the core and the upper 7 m for BH 11 and BH 10. The TOC and TIC concentrations in the lower portion are lower. For BH 10 lower TOC values may indicate erosion from the carbon deprived sources of environment of the local environment, while for BH 11 most of the carbon might have been lost during long transit in regional rivers. The positive shift in the concentration of carbon at 7 m likely resulted from atmospheric evaporation from the lake surface during a period of lower hydrologic input and drying up conditions, yet interspersed at some point with a short period of higher with higher water input into the lakes. From $\delta^{13}C$ of organic material the landscape of the lower 24 m for both cores hosted C_3-type plants, indicating hydrologically wet interval in the core. The upper part of the cores has enriched values pointing to an environment that is shifting to more arid conditions of the Holocene to the present day. The TOC, TIC and carbon isotopic signatures clearly separate the sediments into two major climatic phases, namely: Phase I and phase II (Figures 6 and 8). Phase I sediments in BH 10 are from a wet climate and are interpreted to have been deposited when the local climate was wet with no water input from regional sources. The carbon was concluded to be sourced from primary production of organic matter from within the megapaleolake hence low MS values. Increasing TOC in the sediments could suggest filling of the lake as more organic carbon is being deposited from multiple sources. Decreasing TOC would suggest limited input from the tropical sources. Isotopic signatures depicts a significant change in vegetation with the values moving to positive

and interpreted as evidence for a changing regional climate of the present day. Phase II for the BH 11 core, TIC concentrations are fluctuating and imply repeated cycles of aridity. TOC values are increasing hence more organic matter input from the landscape into the system. Phase I is a drying climate as depicted from decreased TOC values. Decreasing TOC likely indicates limited vegetation productivity (Meyers, 2003) that may relate to increasing moisture deficiency. Schmidt et al., (2017) concluded that the climate of the middle Kalahari was considered extremely dry with some evidence of short term excursions of significantly higher humidity.

6.4 Paleoenvironmental inferences

The area being investigated forms a part of the Kalahari Basin which is presently covered by Aeolian sediments of predominantly sandy nature. Based on the prominent shift in all the proxies at 6 m depth. Geochemical and magnetic properties analyses of the sediments depict a pattern in climate prompted by strong palaeohydrology of the middle Kalahari basin that gave rise to Mababe Depression, Makgadikgadi Pan and Lake Ngami (Burrough et al., 2009; Diaz et al., 2019). The differences in geochemical proxies' patterns resulted from wet and dry climate cycles between the Pleistocene (wet) and the Holocene (dry).

Sediments physical and chemical properties, as well as their organic carbon isotopic composition from two localities in the northwest revealed evidence of extensive lake systems occupied areas that extended into the lower parts of the present-day Okavango Delta as proposed by Thomas and Shaw (1991; 2002).

The results showed the different depositional environments in which the sediments were deposited. The lower 24 m of the stratigraphy at the two study sites revealed sediments that are relatively depleted in $\delta^{13}C_{organic}$ values, while the upper 6 meters are enriched in $\delta^{13}C_{organic}$ values. The differences are interpreted to have resulted from differences in the sediments sources and climate. The lower part represents relatively wet and cool climate while warmer and drier conditions dominated during the deposition of sediments in the upper 7 m of the stratigraphy. Low $\delta^{13}C_{organic}$ correspond to high TOC in BH 11, but not BH 10. A combination of the carbon isotopic data with TOC and conventional source rock proxies such as MS reveals that a low carbon isotopic composition is associated with high TOC and MS values. This shows that sediments with higher MS values were introduced to the paleolakes only during

periods of excessively wet regional climate, suggesting a probable different source with higher concentrations of magnetic minerals.

Successive layers of clay along the core length of BH 11 suggest several episodes of lake high stands, therefore several episodes of wet climate. Periods of wet climate were interspersed with those of short-term aridity when the TIC was concentrated. The changes signify a non-static climate over the length of the core sometimes showing clear intra-climatic variations. The clay rich units in the mid-sections of the core represent a more humid climate and are believed to have accumulated during times of enhanced water and sediments transport into the Middle Kalahari lakes (e.g. Shaw, 1985; 1988; Gumbricht et al., 2001; Huntsman-Mapila et al., 2006; Burrough and Thomas, 2009) through the Okavango-Chobe-Linyanti river system (Thomas and Shaw 1991). The flow has now been impounded by rifting related to the Okavango tectonics (Moore et al., 2012).

From the sediments grainsizes, the spatial position of BH10 within the projected megapaleolake area recorded evidence for the megapaleolake Makgadikgadi as a singular episode of lake high stand, without variation in the lithology, while BH11 showed evidence for megapaleolake Thamalakane as multiple episodic based on the variability in the sizes of grains along the sediments core. The more extensive megapaleolake Makgadikgadi was recorded as a single episode of lake high stand because of very little variation in the sediments physical characteristics, i.e. there is only one continuous layer of sand/silt on the record. On the other hand, periodic layers of clay seen in Borehole 11 indicated multiple episodes of megapaleolake high stands. The clays contain TIC deposition, indicating that the lake high stands were occasionally interrupted by periods of short term aridity. The sediments granulometry show greater vertical variability owing to periodically changing depositional environments from lacustrine to aridity. The finer sediments in BH 11 support lacustrine deposition, and that a lake once existed at these locations. The combined interpretation of the two cores suggests that megapaleolake Makgadikgadi existed only once and that was before the onset of rifting in the Okavango. Meanwhile, the younger and smaller megapaleolake Thamalakane existed several times in the past. Aeolian deposition predominated in the upper 6 meters of both cores where silts and clays that are characteristic of sand dune deposits of the Kalahari environment contain heavier $\delta^{13}C_{organic}$ values typical of the present-day climate.

6.5 Recommendations

This study was based on a core length of 30 m sampled once every 1 m. This resolution is a limitation and it is recommended that a more detailed study with reduced interval of sampling would be more ideal, and would yield more reliable conclusions. Another disadvantage of the study was that the samples were collected as drill chips making them highly prone to cross contamination. Continuous cores of undisturbed samples would immensely improve on the current results as well as on the interpretations for past climate. More importantly is the proper timing of events that requires dating to be done on the sediments. With dating a more complete sequence of events with their ages would be useful especially in resolving the still lingering question of initiation and timing of rifting in the lower Okavango.

REFERENCES

Brenner, M., Whitmore, T. J., Curtis, J. H., Hodell, D. A., & Schelske, C. L. (1999).Stable isotope ($\delta^{13}C$ and $\delta^{15}N$) signatures of sedimented organic matter as indicators of historic lake trophic state. Journal of Paleolimnology, 22 (2), 205–221.

Bufford, K. M., Atekwana, E. A., Abdelsalam, M. G., Shemang, E., Atekwana, E. A.,Mickus, K., Molwalefhe, L. (2012). Geometry and faults tectonic activity of the Okavango Rift Zone, Botswana: Evidence from magnetotelluric and electrical resistivity tomography imaging. Journal of African Earth Sciences, 65, 61–71.

Burrough, S. L., and Thomas, D. S. (2009). Geomorphological contributions to palaeolimnology on the African continent. Geomorphology, 103 (3), 285–298.

Burrough, S. L., Thomas, D. S., & Bailey, R. M. (2009). Mega-lake in the Kalahari: A Late Pleistocene record of the Palaeolake Makgadikgadi system. Quaternary Science Reviews, 28 (15-16), 1392–1411.

Burrough, S. L., Thomas, D. S., Shaw, P. A., & Bailey, R. M. (2007). Multiphase Quaternary highstands at Lake Ngami, Kalahari, northern Botswana. Palaeogeography, Palaeoclimatology, Palaeoecology, 253 (3-4), 280–299.

Chiverrell, R., Oldfield, F., Appleby, P., Barlow, D., Fisher, E., Thompson, R., & Wolff, G. (2008). Evidence for changes in Holocene sediment flux in SemerWater and Raydale, North Yorkshire, UK. Geomorphology, 100 (1-2), 70–82.

Clark, I., & Fritz, P. (1997). Tracing the carbon cycle. Environmental Isotopes in Hydrogeology, 111–134.

Cooke, H., & Verstappen, H. T. (1984). The landforms of the Western Makgadikgadi Basin in northern Botswana, with a Consideration of the Chronology of the Evolution of Lake Palaeo-Makgadikgadi. Zeitschrift Für Geomorphologie, 28, 1–19.

Dearing, J. (1997). Sedimentary indicators of lake-level changes in the humid temperate zone: a critical review. Journal of paleolimnology, 18 (1), 1–14.

Dearing, J. A., and Jones, R. T. (2003). Coupling temporal and spatial dimensions of global sediment flux through lake and marine sediment records. Global and Planetary Change, 39 (1-2), 147–168.

Diaz, N., Armitage, S. J., Verrecchia, E. P., & Herman, F. (2019). OSL dating of a carbonate island in the Chobe Enclave, NW Botswana. Quaternary Geochronology, 49, 172-176.

Ellery, W. N., McCarthy, T. S., & Smith, N. D. (2003). Vegetation, hydrology, and sedimentation patterns on the major distributary system of the Okavango fan, Botswana. Wetlands, 23 (2), 357–375.

Ellwood, B. B., Tomkin, J. H., Ratcliffe, K. T., Wright, M., & Kafafy, A. M. (2008). High-resolution magnetic susceptibility and geochemistry for the Cenomanian/Turonian boundary GSSP with correlation to time equivalent core. Palaeogeography, Palaeoclimatology, Palaeoecology, 261 (1-2), 105–126.

Fields, A. M. (2012). Investigating Paleoflooding in the Okavango Delta from Sedimentary Records, Northwest Botswana. M.S. Thesis, Oklahoma State University.

Foster, G., Chiverrell, R., Harvey, A., Dearing, J., & Dunsford, H. (2008). Catchment hydro-geomorphological responses to environmental change in the Southern Uplands of Scotland. The Holocene, 18 (6), 935–950.

Gamrod, J. L. (2009). Paleolimnological records of environmental change preserved in Paleo-lake Mababe, Northwest Botswana. M.S. Thesis, Oklahoma State University.

Giguet-Covex, C., Arnaud, F., Poulenard, J., Disnar, J.-R., Delhon, C., Francus, P., Delannoy, J.-J. (2011). Changes in erosion patterns during the Holocene in a currently treeless subalpine catchment inferred from lake sediment geochemistry (Lake Anterne, 2063 m asl, NW French Alps): the role of climate and human activities. The Holocene, 21 (4), 651–665.

Grove, A. T. (1969). Landforms and climatic change in the Kalahari and Ngamiland. The Geographical Journal, 135 (2), 191–212.

Gumbricht, T., McCarthy, T., & Merry, C. L. (2001). The topography of the Okavango Delta, Botswana, and its tectonic and sedimentological implications. South African Journal of Geology, 104 (3), 243–264.

Gumbricht, T., Wolski, P., Frost, P., & McCarthy, T. (2004). Forecasting the spatial extent of the annual flood in the Okavango Delta, Botswana. Journal of Hydrology, 290 (3-4), 178–191.

Håkanson, L., Jansson, M., (1983). Principles of Lake Sedimentology Blackburn Press, USA.

Hamandawana, H., Chanda, R., & Eckardt, F. (2008). Reappraisal of contemporary perspectives on climate change in Southern Africa's Okavango Delta sub-region. Journal of Arid Environments, 72 (9), 1709–1720.

Hayes, J. M. (2004). An introduction to isotopic calculations. Woods Hole Oceanographic Institution, Woods Hole, MA, 2543.

Hayes, J. (1993). Factors controlling ^{13}C contents of sedimentary organic compounds: Principles and evidence. Marine Geology, 113 (1-2), 111–125.

Hodell, D. A., & Schelske, C. L. (1998). Production, sedimentation, and isotopic composition of organic matter in Lake Ontario. Limnology and Oceanography, 43 (2), 200–214.

Hollander, D. J., & McKenzie, J. A. (1991). CO_2 control on carbon-isotope fractionation during aqueous photosynthesis: A Paleo-PCO_2 barometer. Geology, 19 (9), 929–932.

Hollander, D. J., McKenzie, J. A., & Haven, H. L. t. (1992). A 200 year sedimentary record of progressive eutrophication in Lake Greifen (Switzerland): implications for the origin of organic-carbon-rich sediments. Geology, 20 (9), 825–828.

Huntsman-Mapila, P., Kampunzu, A., Vink, B., & Ringrose, S. (2005). Cryptic indicators of provenance from the geochemistry of the Okavango Delta sediments, Botswana. Sedimentary Geology, 174 (1-2), 123–148.

Huntsman-Mapila, P., Ringrose, S., Mackay, A., Downey, W., Modisi, M., Coetzee, S., Vanderpost, C. (2006). Use of the geochemical and biological sedimentary record in establishing palaeo-environments and climate change in the Lake Ngami Basin, NW Botswana. Quaternary International, 148 (1), 51–64.

Kinabo, B. D., Atekwana, E. A., Hogan, J. P., Modisi, M. P., Wheaton, D. D., & Kampunzu, A. (2007). Early structural development of the Okavango Rift Zone, NW Botswana. Journal of African Earth Sciences, 48 (2-3), 125–136.

Kling, G. W., Kipphut, G. W., & Miller, M. C. (1991). Arctic lakes and streams as gas conduits to the atmosphere: implications for tundra carbon budgets. Science, 251 (4991), 298-301.

Knight, J. and Fitchett, J.M., 2019. Climate Change during the Late Quaternary in South Africa, The Geography of South Africa. Springer, 37-45.

Koinig, K. A., Shotyk, W., Lotter, A. F., Ohlendorf, C., & Sturm, M. (2003). 9000 years of geochemical evolution of lithogenic major and trace elements in the sediment of an alpine lake–the role of climate, vegetation, and land-use history. Journal of Paleolimnology, 30 (3), 307–320.

Kranz, N., & Vorwerk, A. (2007). Public participation in transboundary water management. In Amsterdam conference on the human dimensions of global environmental change (Vol. 30).

Krishnamurthy, R., Atekwana, E. A., & Guha, H. (1997). A simple, inexpensive carbonate- phosphoric acid reaction method for the analysis of carbon and oxygen isotopes of carbonates. Analytical Chemistry, 69 (20), 4256–4258.

Kump, L. R., & Arthur, M. A. (1999). Interpreting carbon-isotope excursions: carbonates and organic matter. Chemical Geology, 161 (1-3), 181–198.

Lario, J., Spencer, C., Plater, A., Zazo, C., Goy, J., & Dabrio, C. (2002). Particle size characterisation of holocene back-barrier sequences from North Atlantic coasts (SW Spain and SE England). Geomorphology, 42 (1-2), 25–42.

Leng, M. J., & Marshall, J. D. (2004). Palaeoclimate interpretation of stable isotope data from lake sediment archives. Quaternary Science Reviews, 23 (7-8), 811-831.

Liu, H., Xu, L., & Cui, H. (2002). Holocene history of desertification along the woodland-steppe border in Northern China. Quaternary Research, 57 (2), 259–270.

Lowe, J., and Walker, M.C. (1997). Reconstructing quaternary environments 2nd edition. Addison Wesley Longman Ltd, Essex.

MacDonald, G., Felzer, B., Finney, B., & Forman, S. (2000). Holocene lake sediment records of Arctic hydrology. Journal of Paleolimnology, 24 (1), 1-13.

Mackereth, F.J.H., (1966). Some chemical observations on post-glacial lake sediments. Philos. Trans. R. Soc. B Biol. Sci. 250, 165–213.

McCarthy, T. (2013). The Okavango Delta and its place in the geomorphological evolution of Southern Africa. South African Journal of Geology, 116 (1), 1–54.

McCarthy, T., and Ellery, W. (1998). The Okavango Delta. Transactions of the Royal Society of South Africa, 53 (2), 157–182.

McCarthy, T. S., Smith, N. D., Ellery, W. N., & Gumbricht, T. (2002). The Okavango Delta—semiarid alluvial-fan sedimentation related to incipient rifting.

McFarlane, M., and Eckardt, F. (2008). Lake deception: A new Makgadikgadi Palaeolake. Botswana Notes and Records, 38, 195–201.

Meyers, P.A., (2003). Applications of organic geochemistry to paleolimnological reconstructions: a summary of examples from the Laurentian Great Lakes, Organic Geochemistry, 34, 261-289.

Meyers, P. A., and Ishiwatari, R. (1993). Lacustrine organic geochemistry-An overview of indicators of organic matter sources and diagenesis in lake sediments. Organic geochemistry, 20 (7), 867–900.

Meyers, P. A., and Teranes, J. L. (2002). Sediment organic matter. In Tracking environmental change using lake sediments, 239–269. Springer.

Modisi, M. P., Atekwana, E. A., Kampunzu, A., & Ngwisanyi, T. H. (2000). Rift kinematics during the incipient stages of continental extension: Evidence from the nascent Okavango rift basin, northwest Botswana. Geology, 28 (10), 939–942.

Moore, A., Cotterill, F., & Eckardt, F. (2012). The evolution and ages of Makgadikgadi palaeo-lakes: Consilient evidence from Kalahari drainage evolution South-Central Africa. South African Journal of Geology, 115 (3), 385–413.

Oldfield, F., Barnosky, C., Leopold, E., & Smith, J. (1983). Mineral magnetic studies of lake sediments. In Paleolimnology, 37–44. Springer.

Oldfield, F. (2005). Environmental change: key issues and alternative perspectives. Cambridge University Press.

Oldfield, F., Battarbee, R. W., Boyle, J. F., Cameron, N. G., Davis, B., Evershed, R. P., Walker, R. (2010). Terrestrial and aquatic ecosystem responses to late holocene climate change recorded in the sediments of Lochan Uaine, Cairngorms, Scotland. Quaternary Science Reviews, 29 (7-8), 1040–1054.

Ostroski, M. M. (2013). Investigating the Formation and Evolution of Mega-Paleolakes in the Middle Kalahari of Semi-Arid Botswana from Sedimentary and Geochemical Proxies (Doctoral dissertation, Oklahoma State University).

O'Leary, M. H. (1988). Carbon isotopes in photosynthesis. Bioscience, 38 (5), 328–336.

Parris, A. S., Bierman, P. R., Noren, A. J., Prins, M. A., & Lini, A. (2010). Holocene paleostorms identified by particle size signatures in lake sediments from the north-eastern United States. Journal of Paleolimnology, 43 (1), 29–49.

Riedel, F., Henderson, A. C., Heußner, K. U., Kaufmann, G., Kossler, A., Leipe, C., & Taft, L. (2014). Dynamics of a Kalahari long-lived mega-lake system: hydromorphological and limnological changes in the Makgadikgadi Basin (Botswana) during the terminal 50 ka. Hydrobiologia, 739 (1), 25-53.

Ringrose, S., Huntsman-Mapila, P., Kampunzu, A. B., Downey, W., Coetzee, S., Vink, B., Vanderpost, C. (2005). Sedimentological and geochemical evidence for palaeo-environmental change in the Makgadikgadi subbasin, in relation to the MOZ rift depression, Botswana. Paleogeography, Paleoclimatology, Paleoecology, 217 (3-4), 265–287.

Robinson, M. M., and Dowsett, H. J. (2010). eprism: A case study in multiple proxy and mixed temporal resolution integration. Stratigraphy, 7 (2-3), 177–187.

Schillereff, D. N., Chiverrell, R. C., Macdonald, N., & Hooke, J. M. (2014). Flood stratigraphies in lake sediments: A review. Earth-Science Reviews, 135, 17–37.

Schmidt, M., Fuchs, M., Henderson, A. C., Kossler, A., Leng, M. J., Mackay, A. W., & Riedel, F. (2017). Paleolimnological features of a mega-lake phase in the Makgadikgadi Basin (Kalahari, Botswana) during Marine Isotope Stage 5 inferred from diatoms. Journal of Paleolimnology, *58*(3), 373-390.

Scholz, C. H., Koczynski, T. A., & Hutchins, D. G. (1976). Evidence for incipient rifting in southern Africa. Geophysical Journal International, 44(1), 135-144.

Shaw, P. (1985). Late quaternary landforms and environmental change in northwest Botswana: the evidence of Lake Ngami and the Mababe depression. Transactions of the Institute of British Geographers, 333–346.

Shaw, P. (1988). After the flood: the fluvio-lacustrine landforms of northern Botswana. Earth-Science Reviews, 25 (5-6), 449–456.

Shaw, P. A., Bateman, M. D., Thomas, D. S., & Davies, F. (2003). Holocene fluctuations of Lake Ngami, Middle Kalahari: chronology and responses to climatic change. Quaternary International, 111 (1), 23-35.

Shen, Z., Bloemendal, J., Mauz, B., Chiverrell, R. C., Dearing, J. A., Lang, A., & Liu, Q. (2008). Holocene environmental reconstruction of sediment-source linkages at Crummock Water, English Lake District, based on magnetic measurements. The Holocene, 18 (1), 129–140.

Sperazza, M., Moore, J. N., & Hendrix, M. S. (2004). High-resolution particle size analysis of naturally occurring very fine-grained sediment through laser diffractometry. Journal of Sedimentary Research, 74 (5), 736–743.

Thomas, D. S. G. (1987). Discrimination of depositional environments using sedimentary characteristics in the Mega Kalahari, central southern Africa. Geological Society, London, Special Publications, 35 (1), 293-306.

Thomas, D. S., and Burrough, S. L. (2012). Interpreting geoproxies of late quaternary climate change in African drylands: implications for understanding environmental change and early human behaviour. Quaternary International, 253, 5–17.

Thomas, D. S., & Shaw, P. A. (2002). Late quaternary environmental change in central Southern Africa: new data, synthesis, issues and prospects. Quaternary Science Reviews, 21 (7), 783–797.

Thomas, D., and Shaw, P. A. (1991). The Kalahari environment. Cambridge University Press.

Truc, L., Chevalier, M., Favier, C., Cheddadi, R., Meadows, M. E., Scott, L., & Chase, B. M. (2013). Quantification of climate change for the last 20,000 years from Wonderkrater, South Africa: implications for the long-term dynamics of the Intertropical Convergence Zone. Palaeogeography, Palaeoclimatology, Palaeoecology, 386, 575-587.

Wolfe, B. B., Hall, R. I., Last, W. M., Edwards, T. W., English, M. C., Karst-Riddoch, T. L., Palmini, R. (2006). Reconstruction of multi-century flood histories from oxbow

lake sediments, Peace-Athabasca Delta, Canada. Hydrological Processes, 20 (19), 4131–4153.

Wu, J., Schleser, G. H., Lücke, A., & Li, S. (2007). A stable isotope record from freshwater lake shells of the Eastern Tibetan Plateau, china, during the past two centuries. Boreas, 36 (1), 38–46.

Zhong, W., Xue, J., Li, X., Xu, H., & Ouyang, J. (2010). A holocene climatic record denoted by geochemical indicators from Barkol lake in the Northeastern Xinjiang, NW China. Geochemistry International, 48 (8), 792–800.

APPENDIX A

PHYSICAL CHARACTERISTICS

A1

MUNSELL COLOUR DESCRIPTIONS

A1a: BH 10

SAMPLE DEPTH	MUNSELL COLOUR ID	MUNSELL COLOUR DESCRIPTION
1	10YR 3/1	Very dark gray
2	10YR 5/1	Gray
3	2.5Y 6/1	Gray
4	2.5Y 6/1	Gray
5	2.5Y 6/2	Light brownish gray
6	2.5Y 7/1	Light gray
7	2.5Y 7/2	Light gray
8	2.5Y 7/2	Light gray
9	2.5Y 7/2	Light gray
10	2.5Y 7/2	Light gray
11	2.5Y 7/2	Light gray
12	2.5Y 7/2	Light gray
13	2.5Y 7/2	Light gray
14	2.5Y 7/2	Light gray
15	2.5Y 7/3	Pale yellow
16	2.5Y 7/3	Pale yellow
17	2.5Y 7/3	Pale yellow
18	2.5Y 7/3	Pale yellow
19	2.5Y 6/2	Light brownish gray
20	2.5Y 6/2	Light brownish gray
21	2.5Y 6/2	Light brownish gray
22	2.5Y 6/2	Light brownish gray
23	2.5Y 6/2	Light brownish gray
24	2.5Y 6/2	Light brownish gray
25	2.5Y 6/2	Light brownish gray
26	2.5Y 6/2	Light brownish gray
27	2.5Y 6/2	Light brownish gray
28	2.5Y 6/2	Light brownish gray
29	2.5Y 6/2	Light brownish gray
30	2.5Y 6/2	Light brownish gray

A1b: BH 11

SAMPLE DEPTH	MUNSELL COLOUR ID	MUNSELL COLOUR DESCRIPTION
1	7.5YR 5/2	Brown
2	7.5YR 5/2	Brown
3	10YR 8/2	Very pale brown
4	10YR 6/3	Pale brown
5	10YR 7/3	Very pale brown
6	10YR 7/3	Very pale brown
7	10YR 6/3	Pale brown
8	10YR 7/3	Very pale brown
9	10YR 7/3	Very pale brown
10	10YR 7/3	Very pale brown
11	10YR 7/3	Very pale brown
12	10YR 7/3	Very pale brown
13	10YR 7/3	Very pale brown
14	10YR 7/3	Very pale brown
15	10YR 7/3	Very pale brown
16	10YR 7/3	Very pale brown
17	10YR 6/3	Pale brown
18	10YR 7/3	Very pale brown
19	10YR 7/3	Very pale brown
20	10YR 6/3	Pale brown
21	10YR 7/3	Very pale brown
22	10YR 8/3	Very pale brown
23	10YR 8/2	Very pale brown
24	10YR 8/3	Very pale brown
25	10YR 8/3	Very pale brown
26	10YR 8/3	Very pale brown
27	10YR 8/3	Very pale brown
28	10YR 7/3	Very pale brown
29	10YR 7/3	Very pale brown
30	10YR 6/3	Pale brown

A2

GRAIN SIZES

A2a: BH 10

Depth (m)	Sand (%)	Silt (%)	Clay (%)
0-1	0.16	65.72	34.12
1-2	21.48	56.49	22.03
2-3	40.11	42.11	17.78
3-4	25.25	55.78	18.98
4-5	47.87	38.48	13.66
5-6	67.40	25.27	7.35
6-7	83.29	13.14	3.57
7-8	78.69	16.90	4.42
8-9	91.46	6.70	1.83
9-10	90.28	7.48	2.25
10-11	88.02	9.42	2.56
11-12	91.52	6.59	1.90
12-13	87.61	9.84	2.56
13-14	78.32	17.54	4.15
14-15	85.87	11.22	2.92
15-16	88.85	8.83	2.33
16-17	89.16	8.66	2.19
17-18	91.88	6.44	1.69
18-19	93.81	4.79	1.41
19-20	93.84	4.77	1.40
20-21	91.45	6.75	1.81
21-22	93.30	5.28	1.43
22-23	92.46	5.87	1.67
23-24	90.94	6.98	2.09
24-25	91.83	6.13	2.05
25-26	85.17	11.83	3.02
26-27	88.54	8.83	2.64
27-28	91.35	6.56	2.10
28-29	78.52	16.90	4.59
29-30	74.26	20.08	5.67

A2b: BH 11

Depth (m)	Sand (%)	Silt (%)	Clay (%)
0-1	54.4	35.9	9.7
1-2	61.9	30.1	8.0
2-3	61.3	30.3	8.4
3-4	19.8	64.1	16.1
4-5	70.3	23.8	6.0
5-6	51.8	37.6	10.6
6-7	58.1	32.9	9.0
7-8	64.4	27.6	8.0
8-9	62.5	28.7	8.8
9-10	39.9	47.3	12.8
10-11	61.9	30.1	8.0
11-12	72.2	21.5	6.3
12-13	71.2	22.2	6.5
13-14	63.3	27.8	8.9
14-15	60.9	31.0	8.1
15-16	37.9	46.6	15.6
16-17	72.5	22.1	5.3
17-18	71.6	22.8	5.7
18-19	41.2	45.5	13.3
19-20	56.5	34.0	9.5
20-21	9.5	72.9	17.6
21-22	11.9	70.4	17.7
22-23	35.5	51.6	12.9
23-24	41.1	47.7	11.3
24-25	36.1	50.2	13.7
25-26	41.6	48.1	10.3
26-27	91.4	6.8	1.8
27-28	83.9	13.0	3.1
28-29	82.6	13.6	3.9
29-30	86.9	10.0	3.1

A3

MAGNETIC SUSCEPTIBILITY

A3a: MS BH 10

Depth (m)	Magnetic Susceptibility ($x10^{-8}$) [m^3/kg]
0-1	7.8
1-2	1.7
2-3	1.7
3-4	2.7
4-5	0.8
5-6	0.8
6-7	0.4
7-8	0
8-9	0.8
9-10	0.3
10-11	0
11-12	0.2
12-13	0.8
13-14	0.8
14-15	1.6
15-16	0.5
16-17	0.4
17-18	1.5
18-19	0.8
19-20	0.3
20-21	0
21-22	0.5
22-23	0.3
23-24	0.8
24-25	0
25-26	0.3
26-27	1.5
27-28	1.7
28-29	1.4
29-30	1.7

A3b: MS BH 11

Depth (m)	Magnetic Susceptibility ($x10^{-8}$) [m^3/kg]
0-1	1.1
1-2	1.3
2-3	0.8
3-4	1.6
4-5	1.9
5-6	0.3
6-7	0.8
7-8	7.7
8-9	3.4
9-10	4.1
10-11	0.5
11-12	0
12-13	0.5
13-14	0.9
14-15	0.8
15-16	2.1
16-17	0.9
17-18	0.8
18-19	2
19-20	1.7
20-21	1.4
21-22	1
22-23	0.4
23-24	0.3
24-25	0
25-26	0.7
26-27	0.8
27-28	1.1
28-29	1.2
29-30	1.1

Appendix B

CHEMISTRY DATA

B1: BH 10 Chemistry

DEPTH (m)	TIC (%)	TOC (%)
0-1	0.35	0.45
1-2	0.09	0.23
2-3	0.10	0.17
3-4	1.05	0.16
4-5	0.31	0.05
5-6	0.00	0.03
6-7	0.01	0.04
7-8	0.00	0.03
8-9	0.00	0.04
9-10	0.00	0.01
10-11	0.00	0.01
11-12	0.00	0.01
12-13	0.00	0.02
13-14	0.00	0.01
14-15	0.00	0.01
15-16	0.00	0.02
16-17	0.00	0.01
17-18	0.00	0.02
18-19	0.00	0.01
19-20	0.00	0.01
20-21	0.00	0.00
21-22	0.00	0.00
22-23	0.00	0.00
23-24	0.00	0.00
24-25	0.00	0.00
25-26	0.00	0.00
26-27	0.00	0.00
27-28	0.00	0.00
28-29	0.00	0.00
29-30	0.0	0.00

B2: BH 11 Chemistry

DEPTH (m)	TIC (%)	TOC (%)
0-1	0.00	0.00
1-2	0.00	0.00
2-3	0.07	0.00
3-4	0.13	0.00
4-5	0.04	0.00
5-6	0.00	0.00
6-7	0.09	0.00
7-8	0.00	0.00
8-9	0.06	0.00
9-10	0.00	0.00
10-11	0.07	0.04
11-12	0.09	0.04
12-13	0.12	0.03
13-14	0.09	0.03
14-15	0.05	0.03
15-16	0.18	0.06
16-17	0.01	0.04
17-18	0.05	0.04
18-19	0.00	0.04
19-20	0.05	0.05
20-21	0.00	0.04
21-22	0.00	0.03
22-23	0.00	0.01
23-24	0.00	0.01
24-25	0.00	0.01
25-26	0.00	0.01
26-27	0.00	0.02
27-28	0.01	0.04
28-29	0.00	0.04
29-30	0.00	0.05

APPENDIX C
ISOTOPIC DATA

C1: BH 10

DEPTH (m)	$^{13}C/^{12}C$ (‰)
0-1	-19.65
1-2	-21.70
2-3	-24.64
3-4	-23.66
4-5	-23.83
5-6	-25.06
6-7	-26.67
7-8	-24.85
8-9	-25.19
9-10	-26.01
10-11	-26.42
11-12	-26.63
12-13	-26.54
13-14	-25.98
14-15	-25.55
15-16	-25.83
16-17	-25.98
17-18	-25.11
18-19	-25.66
19-20	-25.84
20-21	-26.89
21-22	-26.53
22-23	-26.36
23-24	-26.26
24-25	-26.51
25-26	-26.30
26-27	-26.48
27-28	-26.31
28-29	-26.34
29-30	-26.05

C2: BH 11

DEPTH (m)	$^{13}C/^{12}C$ (‰)
0-1	-20.58
1-2	-20.48
2-3	-23.58
3-4	-23.22
4-5	-23.86
5-6	-25.36
6-7	-24.51
7-8	-24.71
8-9	-24.84
9-10	-25.41
10-11	-26.03
11-12	-25.85
12-13	-26.04
13-14	-25.63
14-15	-26.02
15-16	-25.63
16-17	-26.72
17-18	-26.40
18-19	-25.92
19-20	-26.06
20-21	-26.90
21-22	-27.16
22-23	-27.37
23-24	-27.18
24-25	-27.24
25-26	-27.15
26-27	-26.88
27-28	-26.67
28-29	-26.31
29-30	-26.30